Helsinki University of Technology
Department of Electrical and Communications Engineering
Laboratory of Electronics Production Technology
Electronics Production Technology Publication Series **HUT-EPT-11**
Espoo 2004

INTERFACIAL COMPATIBILITY OF POLYMER-BASED STRUCTURES IN ELECTRONICS

Markus Turunen

Dissertation for the degree of Doctor of Science in Technology to be presented with due permission of the Department of Electrical and Communications Engineering, Helsinki University of Technology, for public examination and debate in Auditorium S4 at Helsinki University of Technology (Espoo, Finland) on the 1st of October, 2004, at 12 noon.

SUPERVISOR

Professor Jorma Kivilahti, D.Sc. (Tech)
Department of Electrical and Communications Engineering
Laboratory of Electronics Production Technology
Helsinki University of Technology

REVIEWERS

Senior Research Manager Jukka Rantala, Dr.
Nokia Research Center
Helsinki, Finland

Professor Raymond A. Pearson, Dr.
Materials Science & Engineering Department
Center for Polymer Science and Engineering
Lehigh University
Bethlehem, United States of America

OPPONENT

Professor C. P. Wong, Dr.
Materials Science and Engineering
Georgia Institute of Technology
Atlanta, United States of America

Distribution:
Helsinki University of Technology
Department of Electrical and Communications Engineering
Laboratory of Electronics Production Technology
P. O. Box 3000
FIN-02015 HUT
Finland
Tel: +358 9 451 4989
Fax: +358 9 451 5776
E-mail: Markus.Turunen@hut.fi

ISBN 951-22-7237-7 (printed)
ISBN 951-22-7238-5 (PDF)
ISSN 1457-0440

Espoo 2004
Otamedia Oy

ABSTRACT

Interfacial compatibility of dissimilar materials was investigated to achieve a better understanding of interfacial adhesion in metal/polymer/metal systems. Surface modifications of polymers were applied to improve the adhesion. The modified surfaces were characterised by scanning electron microscopy (SEM), atomic force microscopy (AFM), X-ray photoelectron spectroscopy (XPS) and contact angle measurements accompanied by surface free energy evaluations. The pull-off test was employed to assess the interfacial adhesion strength. Further, to determine the controlling adhesion mechanism, the fracture surfaces exposed in the pull-off test were examined by microscopy. To achieve modification of certain bulk properties of one of the evaluated polymers (SU8 epoxy resin), new star-shaped oligomers were synthesised and reactively blended with it. Oligomers were characterised by ^{1}H and ^{13}C nuclear magnetic resonance (NMR) spectroscopy, Fourier transform infrared (FTIR) spectroscopy, size exclusion chromatography (SEC) and differential scanning calorimetry (DSC). Films of the blends were spin coated on a silicon wafer for characterisation of the refractive index and a novel non-destructive method was developed to measure selected thermal properties of the films. The information concerning interfacial compatibility obtained in this work is of great practical as well as theoretical importance.

PREFACE

The work for this thesis was carried out in the Laboratory of Electronics Production Technology at Helsinki University of Technology between January 2000 and December 2003. Financial support was received through research projects funded by the Academy of Finland and the National Technology Agency (TEKES) and through the Graduate School of Electronics Manufacturing funded by the Ministry of Education. I am most grateful to my supervisor, Professor Jorma Kivilahti, for his counselling in regard to both theoretical and practical aspects of this thesis. The important and essential instruction he provided was invaluable in completing the work while his enthusiasm for finding seminal applications for new materials and understanding them in detail was a constant source of inspiration. During the years spent researching this subject I have accumulated a wealth of knowledge and experience.

The following people, both professionally and personally, have contributed towards the completion of this thesis: my co-authors, Dr. Kari Lounatmaa, Pia Holmberg, Dr. Kathleen Ahonen, Pirjo Kontio, Dr. Paul Starck, Laura Orre, Ari Kuisma, Pekka Marjamäki, Vesa Vuorinen, Risto Hienonen and Andrei Olykainen. Colleagues in our lab and the collaborating labs are thanked for providing, a pleasant and inspiring working atmosphere, plus many enjoyable and unforgettable moments both during and after working hours. Dr. Tomi Laurila, Toni Mattila and Tapio Saarinen have contributed to the work not only as colleagues but also as friends and formidable competitors in the gym. Indeed, I want to thank all my friends for the constant interest they have shown in the progress of my work and, in particular, for many great times together. Please accept my heartfelt gratitude; I owe you a lot.

My parents Elli and Aarne are deserving of special thanks, for providing continuous support, admirable endurance and endless faith in me. Thanks go also to sister Anne-Marja and my relatives. Finally, I remember with warmest gratitude my grandparents, Maire and Veikko†, in whose good company I spent most of my childhood summers learning countless wise things about life.

Nastola, April 2004

Markus Turunen

CONTENTS **Page**

LIST OF ABBREVIATIONS AND SYMBOLS

AFM	Atomic force microscopy
BEI	Backscattered electron image
CL	ε-Caprolactone
CTE	Coefficient of thermal expansion
DMA	Dynamic mechanical analysis
DSC	Differential scanning calorimetry
EDS	Energy dispersive X-ray spectrometry
FEM	Finite element method
FE-SEM	Field emission scanning electron microscopy
FMG	Flowing mixed gas
FTIR	Fourier transform infrared
HDI	High density interconnection
IA	Itaconic anhydride
IC	Integrated circuit
IEC	International Electrotechnical Commission
IMB	Integrated module board
IMFP	Inelastic mean free path
LCP	Liquid crystal polymer
MA	Maleic anhydride
MWD	Molecular weight distribution
NMR	Nuclear magnetic resonance
OH	Hydroxyl group
PCL	Poly(ε-caprolactone)
PGL	Polyglycerol
ppb	Parts per billion
ppm	Parts per million
PWB	Printed wiring board
RF	Radio frequency
RH	Relative humidity
RIE	Reactive ion etching
SA	Succinic anhydride
SEC	Size exclusion chromatography

SEI	Secondary electron image
$SnOct_2$	Stannous octoate, Sn(II)2-ethylhexanoate
SPM	Scanning probe microscopy
STM	Scanning tunnelling microscopy
SU8	Eight functional photodefinable epoxy resin
WDS	Wavelength dispersive X-ray spectrometry
XPS	X-ray photoelectron spectroscopy
Z	Atomic number

A	Pre-exponential factor in Arrhenius equation
B_0	External magnetic field in NMR instrument
B_1	RF pulse in NMR instrument
d	Thickness
E	Elastic modulus
E_A	Activation energy
E_b	Binding energy of electron in atom
E_k	Kinetic energy of electron
E_α	Activation energy at conversion α
$f(\alpha)$	Reaction model as a function of α
G	Toughness
G_c	Fracture toughness
hv	Energy of the X-ray source
I	Current
I_0	Intensity
I_d	Intensity at the depth d
I_n	Atomic spin number
I_Z	Atomic spin state
k	Reaction rate constant
K_α	Characteristic X-ray radiation
$\overline{M}_i$	Net magnetic moment in direction i
$\overline{M}_n$	Number averaged molecular weight
n	Refractive index
Q	Heat

R	Gas constant
T	Temperature
t	Time
T_g	Glass transition temperature
T_m	Melting temperature
w	Work function in XPS detector
W_i	Work of adhesion for component *i*
ΔH_r	Reaction enthalpy
α	Conversion
β	Heating rate
γ_i	Surface free energy for component *i*
δ	Tensile strength
ε	Strain
θ	Contact angle
θ_e	Equilibrium contact angle
θ'	Angle of incidence in XPS
θ_t	Take of angle in XPS
λ	Wavelength
μ	Magnetic moment of spinning atom
π	Spreading pressure
υ	Poisson ratio
$\varnothing'$	Angle between the normal of the film and the ray of reflected light

LIST OF PUBLICATIONS

I Markus P.K. Turunen, Tomi Laurila, Jorma K. Kivilahti, ”Evaluation of the surface free energy of spin-coated photodefinable epoxy”, *Journal of Polymer Science: Part B: Polymer Physics,* **40,** (2002), 2137-2149.

II Markus P.K. Turunen, Pekka Marjamäki, Matti Paajanen, Jouko Lahtinen, Jorma K. Kivilahti, ”Pull-off test in the assessment of adhesion at printed wiring board metallisation/epoxy interface”, *Microelectronics Reliability,* **44,** (2004), 993-1007.

III Jun Ge, Markus P.K. Turunen, Jorma K. Kivilahti, ”Surface modification and characterisation of photodefinable epoxy/copper systems”, *Thin Solid Films,* **440 (1-2),** (2003), 198-207.

IV Jun Ge, Markus P.K. Turunen, Maja Kusevic, Jorma K. Kivilahti, ”Effects of surface treatments on adhesion of copper to a hybrid polymer material”, *Journal of Materials Research,* **18,** (2003), 2697-2707.

V Jun Ge, Markus P.K. Turunen, Jorma K. Kivilahti, “Surface modification of a liquid crystalline polymer for copper metallisation”, *Journal of Polymer Science: Part B: Polymer Physics,* **41,** (2003), 623-636.

VI Markus P.K. Turunen, Harri Korhonen, Jukka Tuominen, Jukka V. Seppälä, ”Synthesis, characterisation and crosslinking of functional star-shaped poly(ε-caprolactone)”, *Polymer International*, **51,** (2002), 92-100.

VII Markus P.K. Turunen, Tomi Laurila, Kimmo Solehmainen, Jorma K. Kivilahti, ”Reactive blending approach to modify spin-coated epoxy film”, *Electronics Production Technology Publications Series*, **HUT-EPT-10**, ISSN 1457-0440, ISBN 951-22-7036-6, (2004), 1-42.

Report VII consists of three manuscripts under the general title “Reactive blending approach to modify spin coated epoxy film”. There are three parts: Part I: Synthesis and characterisation of star-shaped poly(ε-caprolactone), Part II: Crosslinking kinetics and Part III: Determination of T_g by spectrophotometry. The manuscripts have been submitted to *Journal of Applied Polymer Science*.

The publications are referred to in the text below by their Roman numerals.

THE AUTHOR'S CONTRIBUTION

The author, together with Professor J.K. Kivilahti, planned the overall research. The manuscripts were exhaustively discussed with Professor Kivilahti. The contribution of the author is described below.

Publication I: Markus Turunen was responsible for the research plan and experimental work. Markus Turunen and Tomi Laurila together interpreted the results and prepared the manuscript.

Publication II: Markus Turunen was responsible for the research plan, experimental work, interpretation of the results and preparation of the manuscript. Matti Paajanen and Jouko Lahtinen carried out the X-ray photoelectron experiments and interpreted these results. Pekka Marjamäki calculated the models of the test set-ups by finite element method.

Publications III-V: Markus Turunen participated in the planning of the research, interpretation of the results and preparation of the manuscripts. Markus Turunen was responsible for the contact angle measurements, which were carried out at Ashland Speciality Chemicals, Porvoo, Finland.

Publication VI: Markus Turunen was responsible for the research plan, experimental work and preparation of the manuscript. Markus Turunen, Harri Korhonen and Jukka Tuominen were jointly responsible of the interpretation of the results.

Publication VII: Markus Turunen was responsible for the research plan, experimental work, and interpretation of the results. Kimmo Solehmainen carried out the spectrophotometer characterisation and participated in the preparation of the report. Markus Turunen and Tomi Laurila were jointly and mainly responsible for the preparation of the report.

1 INTRODUCTION

1.1 General background

Today's consumers are demanding highly reliable electronic devices for an increasing number of applications. Manufacturers have been meeting the demands by providing compact products with ever-more versatile functions. The result has been a significant and continuing miniaturisation of electronics, requiring the use of smaller components and a reduction in power consumption. High-density interconnection (HDI) boards are playing an increasing role, as are modular assembly and the utilisation of higher frequencies.[1,2] High-density interconnection and packaging technologies are becoming available.[3-7] The manufacturing of advanced electronics will be truly established, however, only through the development and implementation of innovative materials and production solutions. One such production solution is to integrate silicon chips and passive components with high-density copper wiring into build-up substrates.[8] This can be done by fully additive or semiadditive techniques utilising photodefinable polymers and chemical metal-deposition processes.[9,10,11]

Signal integrity problems and other limitations encountered in high-frequency applications, demand the use of innovative materials[12,13] and optical components and interconnections.[14-16] Technologies tying together the optical and electrical functions into opto/electronic modules appear highly attractive and are gaining in importance.[17] Adoption of the techniques familiar in microlithographic processing together with new optical-grade polymers enables the fabrication of embedded optical waveguides and optical interconnections into HDI substrates.[18,19] The embedding of optical waveguides and interconnections in HDI PWBs in turn demands the use of surface-mounted optoelectronic components. These can only be realised, however, through the employment of expensive, high accuracy alignment processes. Greater focus on interfacial reliability is also demanded.[20,21] It needs to be underlined, however, that the technological advantages provided by highly integrated electronic and opto/electronic build-up modules depend not only on advanced materials and fabrication processes but also–and often primarily–on good adhesion between thin layers of dissimilar materials.[13,22,23, I-V]

Build up of functional electronic devices requires the use of a variety of advanced materials. In both electronic components and assemblies, many interfaces will be required between chemically, physically and mechanically dissimilar materials. The dissimilar properties of metals, polymers, ceramics and composites are likely to give rise to many different failure modes during

operation.[24] Maintaining of the interfacial adhesion in changing environments and tailoring of material properties to provide interfacial compatibility are thus of crucial importance.

The fabrication of highly miniaturised electronic modules through the embedding of integrated circuits, passive components and optical waveguides into PWBs can be expected to lead to revolutionary new products in the fields of electronics, welfare technology and the life sciences. The conventional prerequisites for good interfacial compatibility are thus being expanded to cover the mastery of biointerfaces (living tissue/synthetic material). Every effort made to understand interfacial compatibility will thus assist the reliable fabrication of consumer products based on novel manufacturing technologies and, advanced and tailor-made materials. The modification and characterisation of the properties of surfaces is thus of great practical significance.

1.2 Scope of the study

Novel interconnection techniques have been studied extensively in the Laboratory of Electronics Production Technology at the Helsinki University of Technology.[8-10,25] As the result of an intensive search for reliable, cost-effective and highly miniaturised packaging solutions, the Integrated Module Board (IMB) interconnection technology was established at the end of the nineties and is now being implemented in production by Imbera Electronics. The technology provides for the solderless fabrication of ultra-high density modules using embedded active and passive components. The embedding of optical waveguides into opto/electronic build-up modules has been intensively studied as well.[18,19]

The objective of the present work was to obtain a better understanding of interfacial compatibility, which is one of the major reliability-related concerns of advanced electronics. To meet this objective, selected interfaces of opto/electronic build-up modules were manipulated and investigated. The physical and chemical changes induced by the modifications of various polymer and copper surfaces were investigated and, more specifically, the effect of the roughness and chemical nature of the surfaces on the interfacial adhesion in copper/polymer systems was clarified. Since interfacial adhesion is affected in a major way by the properties of the materials, there is a need to modify existing materials to meet interfacial compatibility requirements. With a view to tailoring the thermomechanical and optical properties of polymers, novel star-shaped network precursors were synthesised, thoroughly characterised and reactively blended with SU8 epoxy resin. For in-depth characterisation of films prepared of this blend, a model-free kinetic analysis was undertaken and a novel method was introduced to determine, non-destructively and *in situ,* selected thermal properties of polymer films in the range of a few micrometres.

The overview that follows provides background information relevant to the work reported in the appended Publications I-VII. The most important methods and practices needed to achieve the objective of the work are discussed in detail. Chapter 2 deals with polymer characteristics of special relevance for the work. In chapter 3, the concept of interfacial adhesion is discussed and chapter 4 deals with the experimental methods used in the work. The most significant findings and conclusions of the work are summarised in a short final chapter.

2 POLYMERIC MATERIALS IN ELECTRONICS

Polymer-based materials have become ubiquitous in a variety of high-tech applications, speciality coatings, automotive parts, aerospace materials, semiconductors, composites and optical materials. In the field of electronics, there is a growing trend to utilise polymeric materials at various levels in the fabrication of advanced devices. Polymers offer a wide variety of chemical and physical properties appropriate for numerous applications. Relative to metals and ceramics, polymers are also cost-effective, lightweight and easily processable. Most of all, many polymer properties can be extensively tailored to meet the specific requirements set by a given application.

Traditionally polymers have been used in electronics as PWB materials and photo resists in microelectronics. Active components fabricated in microelectronics are usually encapsulated in polymer packages to hinder moisture ingress and reduce mechanical loads therefore ensuring reliable performance of the components assembled on PWBs.[26] The use of polymers has established technologies that utilise conductive adhesives[25,27] and flip-chip assembly. The flip-chip assembly requires the employment of polymeric underfill materials that provide mechanical support to the solder joints.[28-30] Optical waveguides and interconnections can be produced from polymers and can be integrated into PWBs utilising e.g. photolithographic processing of polymers adopted from microelectronics.[17,31] Despite the many uses of polymers in electronics, there are at least two basic requirements for the manufacture of all functional assemblies and modules involving polymers. These are the controlled adhesion of the polymer to many other materials in build-up layers,[5] adhesive joints,[32] solder balls,[33,34] solder masks on PWBs,[35] the passivation layer of IC,[35] lead frames,[36] dies[37] and optical waveguides[18,19] and the controlled release of polymers like IC packages from encapsulation moulds.[38]

For the future, the increasing employment of polymers in the manufacture of electronic devices will enable new applications not only in the field of electronics but also in the life sciences establishing for example, lab-on-a-chip instruments.[39,40] These developments will not take place,

however, without in-depth research and technological breakthroughs in many areas, including the manipulation of surface properties.[41-43]

2.1 Structure-property relationship

The constantly expanding use of polymer-based materials has highlighted the need for a better understanding of their physical, chemical and mechanical properties. The properties of a polymer are primarily defined by its chemical composition and molecular architecture. The size of the polymer molecule also affects significantly properties like viscosity, as well as thermal, mechanical and chemical stability. The chain mobility or rigidity of a polymer is determined by the monomers used in the synthesis, which have, therefore, a direct influence on several properties of the polymer. Copolymerisation is a common way to alter the characteristics of polymers.[44,45] Recently, however, considerable emphasis has been placed on tailoring of the molecular architecture instead of the chain chemistry.[46-47] The simplest polymer of all is polyethylene, in principle a linear chain composed of ethylene monomers. The introduction of branches along the polymer chain has significant influence on the processability of a polymer.[49] More importantly, the introduction of branches increases the number of end-groups, or functional groups as they are often called when they differ chemically from the main structure of a the polymer. The functional groups affect various properties, and among other things, can be used to tailor surface properties.[43] The effect of functional groups on properties is more pronounced for low-molecular-weight polymers, which are called oligomers. Here, the term star-shaped oligomer is used to describe a polymer architecture that has several branches radiating out a core molecule.[VI,VII]

The crystallinity of an oligomer decreases as the number of branches increases, evidently because the free chain ends disturb the formation of ordered structure. This becomes reflected, in particular, in the rheological, mechanical, thermal and surface properties of the polymer. In addition, the toughening of inherently brittle polymers through blending with highly branched polymers is reported to be especially effective.[50]

The technical properties of a thermosetting polymer evolve as a function of crosslinking. Crosslinking density is a measure of molecular weight between the covalent bonds that tie together the network precursors, i.e. the oligomers of a resin. Hence, the smaller the oligomer and the higher its functionality, the higher is *the density of crosslinking*. It is to be noted that *the degree of crosslinking* is the measure of the conversion of those reactive groups that transform into the crosslinks and thus it describes the network differently than the density of crosslinking.

Polymeric materials are characterised by two major transition temperatures–crystalline melting (T_m) and glass transition (T_g). The T_g is particularly important because it marks the temperature at which a number of physical properties of the polymer change. Above T_g the amorphous domains of a polymer are said to be in a rubbery state and below it in a glassy state. In the transition zone, the free volume of polymer changes significantly and affects various properties. Most of the polymeric materials used in electronics are highly amorphous, which means that the determination of T_g is important.

The use of high frequencies places new demands on dielectric materials.[51] The relative dielectric constant of a polymer should be low to enable fast signal propagation and to minimise signal rise times. The dielectric loss should be low to reduce undesired heat formation, and thus to reduce power consumption. To provide signal integrity, the interface of a conductor and a dielectric material needs to be smooth. Special polymers, e.g. liquid crystalline polymers (LCP), are available for electronics; however, the requirement for smooth interfaces causes problems in respect of interfacial adhesion.[12,V] In some applications the problems associated with the use of electrical conductors at high frequencies can be overcome by replacing conductors with integrated optical waveguides also at PWB level.[17,18,21]

2.2 Surface chemistry

Despite the versatility of polymeric materials, there are some limitations on their application. Often, the surface properties of a polymer will preclude its use, even though its bulk properties are eminently suited for a certain application. Surface modifications, achieved by tailoring the surface properties while retaining other properties, broaden the usefulness of polymers significantly. Examples of modifications are coating applications, where a polymer surface is altered in respect of wetting characteristics and topography. The modifications may profoundly affect the success or failure of interfacial compatibility, whether this involves strong adhesion (e.g. coatings and multilayer PWBs) or inertness (e.g. blood contacting biodevices).

The most frequently used methods for surface modifications in the manufacturing of electronics are presented later in this work and the main effects of the modification treatments are described below. These methods mainly involve chemical surface functionalisation but also to some extent roughening. Functionalisation is usually done to increase the inherently low surface free energy of polymers. This is achieved by the creation of polar functional groups–hydroxyl, carboxyl and amine–to make the surface more hydrophilic. Groups that possess an atom with free valence electrons or an electronegative atom (e.g. oxygen, nitrogen and halogens) will increase the surface

free energy. An exception to the rule comes from symmetry: polytetrafluoroethylene has very low surface free energy even though it is mainly composed of electronegative fluorine atoms. Once the hydrophilic functional groups are produced on the surface they start embedding themselves in the bulk material to minimise the surface free energy.[52] Nevertheless, to an adequate extent, the newly formed functionalities remain on the surface for relatively long times.[III]

2.3 Polymer films

While the behaviour of polymeric molecules in the bulk is essentially known, this is not the case for macromolecules near interfaces. The research on polymeric thin films is focused on thicknesses below 100 nm, though there is also a technological interest in the determination of selected thermal properties of polymeric films in the micrometre thickness range since many functional polymeric films applied in electronics and optoelectronics lie in this range. The polymers usually exist as supported rather than freestanding films and it is often desired that the film characterisation is carried out *in situ* by a non-destructive method.

One property that has been extensively studied in a variety of polymer films is T_g.[53-56] Usually, T_g decreases as the film thickness decreases, but strong interaction between a substrate and the film has the opposite effect on T_g.[57-59] The out-of-plane thermal expansion increases with decreasing film thickness below T_g, but decreases with decreasing film thickness above T_g.[60]

3 INTERFACIAL ADHESION

Interfacial adhesion is a basic demand when build-up modules and electronic devices are fabricated. The Chapter 3 discusses the fundamentals, measuring and durability of interfacial adhesion.

3.1 Concept of interfacial adhesion

Interfacial adhesion can be described as the force needed to separate two bodies along their interface, and it is restricted therefore to the interfacial forces acting across the interface. In practice, a value that purely expresses interfacial adhesion strength can seldom be obtained because several other factors than interfacial forces affect the fracture of the interface during the measurement, and the failure mechanism is of more or less mixed mode. It is nevertheless common to report a value for interfacial adhesion if the fracture path does not penetrate deeply into one of the joint materials. When it does, the failure mechanism is said to be cohesive. Since the failure mechanism and

adhesion strength never depend solely on the forces acting across the interface, the term "practical adhesion" is sometimes favoured. In this thesis the term interfacial adhesion is used except where there was a clear indication of cohesive failure.

Often the surfaces forming an interface belong to two distinct phases of dissimilar materials, but also successive layers of the same material may form a clear interface. In particular, the surface of a crosslinked polymer is chemically different from that of an uncrosslinked resin and the coating of successive layers of thermosetting polymers often results in the formation of an interface. If the first layer is highly crosslinked and also inert towards the next layer, there may be interfacial adhesion problems.

In general, the adhesion between two bodies is the sum of all the interactions that contribute to the holding together of two surfaces. The interactions arise from either mechanical retention or from interatomic forces acting across the interface of the given materials. Also encountered are the formation of covalent and ionic bonds and complex formation across the interface.[61] Mechanical retention arises from either mechanical interlocking of phases or interfacial diffusion of matter. It is to be noted that interfacial diffusion is rare in the case of polymer/metal interfaces but it does occur across a polyimide/copper interface during annealing above the T_g of polyimide[62] and when certain metals are evaporated or sputtered onto polymeric substrates.[63-65] Interfacial adhesion is rarely a result of secondary forces, chemical bonding or mechanical retention alone but is a combination of these.

3.2 Wetting of a solid polymer surface

In most cases, intimate molecular contact at an interface is a necessary requirement for the development of strong interfacial adhesion. This means that the material needs to spread onto the substrate and wet it. Wetting will take place when the surface free energy of the solid substrate is greater than the sum of the surface tension of the liquid and the interfacial free energy. The surface free energy of polymers is comparatively low in relation to that of many other materials and often arise problems in the wetting of solid polymer surfaces. In the case of physical retention by mechanical interlocking, sufficient adhesion may be provided without good wettability, but such an interface is highly susceptible to destructive environmental processes resulting in interfacial failures.

In understanding surface free energy, it is useful to consider a liquid drop resting on a solid surface. In equilibrium and in the absence of any external forces, the drop will spontaneously assume the form of a sphere. This shape corresponds to the minimum surface-to-volume ratio. It

can be assumed that work must be done on the drop to reshape it and therefore increase its surface-to-volume ratio. Also, the molecules in surface are assumed to be at higher energy state than those in the bulk liquid. This can be explained by the fact that a surface molecule has fewer neighbours and, as a consequence, less intermolecular interaction than bulk molecules. There is, then a free energy change associated with the isothermal reversible formation of a liquid surface and this is termed the surface free energy. It must be emphasised that this surface free energy is not the total free energy of the surface molecules but rather the excess free energy that the molecules possess by virtue of their being in the surface.[66-69]

The surface free energy of liquids can be measured directly because the surface formation is reversible and the molecules attain equilibrium almost as soon as a new surface is formed. In principle, all that has been said above for liquids also applies to solid surfaces. In practice, the situation is rather different. When a fresh solid surface is produced, the molecules on the surface will normally be unable (owing to their immobility) to assume their equilibrium configuration. The solid surface so formed has, therefore, a non-equilibrium structure. In addition, the surface free energy of a solid is crucially dependent on the history of the sample including bending of the solid.[70] The surface free energy of solids has to be evaluated indirectly, for example by measuring equilibrium contact angles that a liquid with known surface tension forms with a solid surface.[66-69,71] Contact angle measurements are described in detail in reference 71 and the determination of surface free energy thereof is reviewed in reference 72.

3.3 Kinetics of wetting

So far, wetting has been considered from the viewpoint of thermodynamics. Although the thermodynamics may indicate possible formation of an intimate contact between two phases, the kinetics will more likely be the determining factor for the occurrence of the wetting. We now explore the kinetics of wetting.

3.3.1 Role of surface roughness and capillary action

Roughness will affect the contact angle (θ) of a given liquid on a solid. If the equilibrium contact angle on a smooth surface is less than 90°, roughening the surface will make θ even smaller. This will increase the apparent surface free energy of the solid and thus also the extent of wetting. However, if for a smooth surface θ is greater than 90°, roughening the surface will increase θ and retard wetting. For spontaneous wetting to take place, the equilibrium contact angle of a liquid on a

given smooth surface has to approach zero. Spreading of a liquid on a solid surface may be accelerated by capillary action. Capillary forces effectively utilize fine pores, scratches and other topographical inhomogeneities when a liquid drop forms a contact angle less than 90°.[73-75]

3.3.2 Role of chemical surface homogeneity

A chemically heterogeneous surface contains domains of different surface free energy. The apparent contact angle on a heterogeneous surface is calculated by the Cassie equation.[76] If the heterogeneous domains are very small relative to the size of liquid drop used in the measurement of the contact angle, which is common, it will be difficult to differentiate the influence of the different domains on the contact angle.[77] Even microscale surface heterogeneity has been observed, however, through the use of a special micro droplet condensation technique.[78] In practice, the chemical heterogeneity may result in compromised wetting, varying interfacial adhesion, difficulty in measuring contact angles reproducibly and severe contact angle hysteresis (i.e. the difference between an advancing and a receding contact angle). It has been proposed that the contact angle hysteresis originates from chemical and topographical surface heterogeneity. Many processes taking place on the surface also have an effect on the contact angle, such as adsorption and desorption of the probing liquid, reorientation of functional groups, surface deformation and surface contamination.[79-82]

Although homogeneity of the surface has so far been the desired state, controlled surface heterogeneity may also be of use. Spontaneous orientation and redirection of functional groups can be achieved by applying an external control.[83-85] Orientated and selectively modified surfaces have been utilised to control both the thermodynamics and kinetics of wetting, for example, to enable the build up of nanoscale optical wave guides and fluidic microsystems.[86-88]

3.3.3 Influence of interphasial interactions

Despite the apparent simplicity, the spreading of liquid on solid surfaces may involve many complex physical processes including swelling, dissolution, diffusion and reactions. For a solid polymer surface, it is fairly difficult to study processes like reactive wetting. In metallurgy, in contrast, a great deal has been published on the physical processes that affect the kinetics of wetting.[89-91] An example relevant to electronics is soldering, where the oxidised copper substrate is first reduced by fluxes and then the exposed metal is reactively wetted by a liquid solder that

simultaneously engages in mutual dissolution and interdiffusion with the surface.[92] In this work, the polymer substrates were considered inert towards the probing liquids that were used.

3.3.4 Influence of liquid viscosity

Viscosity describes the flow behaviour of a material. It originates from intermolecular friction, and so hinders spontaneous spreading of liquid over solid surfaces. For adequate wetting, liquids should possess relatively low viscosity at some stage of the processing. Often the intrinsic viscosity is too high and macromolecules are diluted in solvents for viscosity reduction before their use in coating. The use of elevated process temperature is another effective way to enhance wettability. Increased temperature enhances molecular mobility, separating molecules apart from one another, which in turn decreases both viscosity and surface tension of the liquid.[68,69] Nevertheless, thermosetting polymers such as those used as encapsulation and underfill materials start to crosslink during thermal processing, which rapidly increases their viscosity and complicates spreadability.[93]

The spreading kinetics of liquids on solid substrates has been studied simply by monitoring the areal coverage as a function of time;[94] however, theoretical models have been proposed by de Gennes,[89] Tanner,[95] and Seaver and Berg.[96] The models assume that the most significant forces affecting spreading are the liquid's surface tension, which is the driving force, and viscosity, which is the counterforce. The models have been tested[94] and they hold for some cases but not all. In spite of the practical importance of understanding surface phenomena and the theoretical foundation laid by Young and Laplace almost 200 years ago,[69] the surface processes are still poorly understood.[97]

3.4 Measurement of interfacial adhesion

Before starting an adhesion test, it is imperative to gather as much information about the materials as possible. False interpretation is likely if careful consideration is not paid to factors like test geometry and the measurement technique and their suitability to the particular material.

The most common methods for measurement of interfacial adhesion can be divided into the two major categories of tensile and shear tests. However, for testing the adhesion of coatings to substrates, there are a vast number of variations of these basic tests including pull-off, lap joint and peel tests.[98-103] In addition, qualitative methods such as the tape test can be employed for quick evaluation of interfacial adhesion on a fail/pass criterion.[104] Indirect methods such as the cavitation test, have been employed to estimate the adhesion of TiN and similar hard films to substrates.[102,105] It is recognised that the different methods do not provide comparable values of adhesion strength

and sometimes they may even lead to contradictory results.[105] The adhesion tests have been critically discussed in the literature.[23,99-101,106]

The main reason for the selection of the pull-off test in this study was that the stress distribution within the specimens is well controlled. The pull-off test resembles an axially loaded butt joint test, which in turn is a modification of the tensile test. However, every effort has to be made to ensure uniform stress distribution within the pull-off test specimen if the test is to be reliably applied. Shear-type tests, it may be argued, represent best the failure mechanisms found in field applications, but because of the complex stress distribution within the specimen, the design of the test configuration has a pronounced effect on the adhesion strength value obtained.[101] Also the peel test is often used, but it is affected by several experimental parameters (e.g. angle, rate and width of the peel) as well as the bending of flexible foil and friction, all of which dissipate the energy intended to separate the two bodies of interest.[98] The lap shear and peel methods are usually used as comparative tests therefore whereas the pull-off method is used to obtain more comprehensive understanding of the interfacial adhesion.

3.5 Durability of interfacial adhesion

So far, the discussion has focused on the essential role of interfacial adhesion in the manufacture of reliable electronic devices. Of equally great concern is the durability of the adhesion in the changing and often harsh environments to which consumer products are exposed. Destructive processes like corrosion, deformation and fatigue are accelerated by environmental factors, and eventually failures in one form or another will occur. Materials with physically and chemically different properties are frequently combined in electronics, and the interfacial adhesions are thus particularly susceptible to changes in temperature, moisture ingress and mechanical shocks. A fundamental understanding of the interfacial compatibility of dissimilar materials is even more important for the miniature structures of advanced electronics where relatively short times and low stress levels are sufficient to cause problems.

The loss of bulk properties is rarely a reason for the failure of joints attacked by environmental factors. Although the locus of failure of well-prepared joints in adhesion tests is invariably a cohesive fracture in the polymer layer, the exposure of specimen to environmental attacks frequently results in an “apparent” interfacial failure with lowered adhesion strength.[101] This finding underlines the importance of the interface when considering environmental failure mechanisms.

3.5.1 Work of adhesion

In the absence of chemisorption and mechanical retention, the thermodynamic work of adhesion (W) can be used to predict the durability of interfacial adhesion. Although the total absence of these forces is at the interface of metal oxide and a thermosetting polymer unlikely, use of W may still help explain the weakening of interfacial adhesion during the environmental attack of liquids. The work of adhesion in air (W_a) and in the presence of liquid (W_{al}) is given in Equations 1 and 2, respectively.

$$W_a = \gamma_a + \gamma_b - \gamma_{ab} \quad (1)$$

$$W_{al} = \gamma_{al} + \gamma_{bl} - \gamma_{ab} \quad (2)$$

In Equations 1 and 2, the γ_a and γ_b are the surface free energies of the two phases in air (subscript l denotes the properties in liquid) and γ_{ab} is the interfacial free energy. W_a usually has a positive value indicating thermodynamic stability of the interface. In the presence of liquid, however, the thermodynamic work of adhesion, W_{al}, may well have a negative value indicating that the interface is unstable and will dissociate. Indeed, the thermodynamic work of adhesion at metal oxide/epoxy interfaces changes from positive to negative in the presence of water.[101,107] Evidently a significant amount of primary bonds must thus have existed at the copper/epoxy interface studied in Publication II because the epoxy did not delaminate during exposure to the atmosphere at elevated humidity and temperature. These epoxy coatings were prepared on a relatively smooth CuO_2 substrate and only minor statistically insignificant weakening was observed.

To predict the environmental stability of an interface involving primary bonding, a term representing the hydrolytic and thermal stability of the bond should be included in the equation of the work of adhesion. No report of such a model was found in the surveyed literature, however. An investigation of the thermodynamic work of adhesion provides but little help therefore. In fact, it is established practice to expose specimens to accelerated environmental attacks[24] for evaluation of the durability of interfacial adhesion like was done in Publication II.

3.5.2 Environmental stability assessment of interfacial adhesion

Since the expected operational time of an electronic device is measured in years, accelerated tests must be employed to assess the interfacial reliability within a reasonable period of time. Several accelerated tests are used to induce failure modes resembling those occurring in normal use.[24,108] The response of polymeric material to the stresses caused by environmental attacks is discussed in Publication II and in the literature.[32,106,109] The use of accelerated tests in reliability assessment is not always straightforward, however, because the environments used to achieve the acceleration effect may lead to unrepresentative failure mechanisms and therefore to very misleading results.[32,110]

4 EXPERIMENTAL METHODS

In the Chapter 4, an overview of procedures employed to meet the target of this work is given and the most important characterisation and evaluation methods used in the work reported in Publications I-VII are discussed.

4.1 Experimental procedures

The sections below describe the procedures used in the present work in the order they appear in Publications I-VII.

4.1.1 Surface modifications

Most polymers have low surface free energy and are not amenable to interfacial adhesion without a change in their inherent surface chemistry. Modification of polymer surfaces can be carried out without altering the bulk properties. However, the affected layer will then differ significantly, in both physical and chemical properties, from the bulk material. Often the roughness of the surface is increased as well. The thickness of the affected layer varies with the material, but usually the modification reaches into the first few micrometres.

Although are many techniques are available for polymer surface modification, they can effectively be divided into the two major categories of wet and dry processing. In wet processes, polymers are immersed in chemical solutions, where as in dry processes they are subjected to vapour-phase species. Dry processing basically involves a bombardment from above the sample,

during which the reactive species travels along the direction of an electric field established between electrodes above and beneath the sample. Unlike the wet processing, this results in a mountain-like topography without significant creation of cavities. Both wet and dry processes were applied in this work.

Wet processing is composed of three stages: swelling, etching and neutralising. The purpose of the swelling is to make the topmost surface layer susceptible towards the etching solution. The time used for swelling determines the depth of the resulting modification. The swelling solution diffuses into the surface layer and softens it by plasticisation. The $KMnO_4$ component of etching solution will then readily diffuse into the swelled layer and attack the material through oxidation of the polymer molecules. Oxidation breaks the polymer molecules into small molecular weight fragments, which dissolve in the solution. Oxygen is incorporated into the remaining chains through the creation of new functional groups like hydroxyl and carboxyl. If, and only if, there is more than one phase in the polymer material, a microporous surface can be achieved. The oxidative treatment can also be applied without prior swelling to obtain a plain chemical modification of the surface with minimised roughening effect. The use of swelling solution accelerates the etching rate even with homogeneous polymers, but with heterogeneous polymers an appropriate swelling treatment ensures different etching rates in the various phases providing that there is a difference in their chemical stability. It needs to be mentioned that prolonging the etching treatment endlessly does not have an effect on the modification depth or the degree of oxidation. This is because the redox reaction that takes place during etching yields MnO_2 deposits on the polymer, which effectively inhibit diffusion of the reactive $KMnO_4$ into the polymer and thus prevent the oxidative etch-reaction from continuing. This MnO_2 layer is finally removed in the neutralizing solution.[111,112]

Dry processing etches surfaces through the use of chemically reactive gases or through a physical bombardment of gaseous atoms that resembles sandblasting. Reactive ion etching (RIE) involves both chemically reactive species and physical bombardment to provide anisotropic etching with fast rate, whereas plasma etching is based on the use of chemically reactive species alone.[113,114] The detailed process parameters used in this work for RIE are given in Publications I, IV, V. Two kinds of plasma etching systems are in use: the barrel (cylindrical) and the parallel plate (planar) systems. They operate on the same principles but vary in configuration. The barrel type of reactor was used here, and the operating parameters and configuration specifics are given in detail in Publications III-V. In barrel plasma reactors, radio frequency (RF) energy ionises the employed gas and forms the plasma. The dominant etch mechanism relies on the reactive species of the plasma because the ion bombardment can be inhibited by the perforated metal tunnel that provides a shield between the plasma source and the sample. Reactive species are absorbed onto the surface where

they form volatile etch products that are eventually desorbed from the surface and removed by a vacuum pump. Since the energies of ions are relatively low, etch rates in the vertical and lateral directions are often similar, resulting in an isotropic etching unless there are several phases in the treated material.

Homogeneous polymers remain reasonably smooth regardless of the method used in their modification. Polymer blends in which reaction induced phase separation occurs during a crosslinking bake are particularly prone to obtain a microporous surface during treatment if one of the separated phases is chemically weaker toward the etching medium than the other(s). The main consequences of plasma exposure are the removal of organic material and the oxidation of the remaining polymer surface. The same takes place in RIE, but there ion bombardment is usually dominant over the chemical etching and the resulting surface is topographically changed rather than chemically altered. The difference is illustratively shown in Publication V.

4.1.2 Metallisation methods

Once the polymer surface has been adequately modified, it can be metallised by various techniques. Electroless plating and sputter deposition produce thin metallisation layers, whereas electroplating results in relatively thick layers. Electroplating follows often electroless plating or sputter deposition. In this work, the interfaces of interest were produced by electroless and sputter-deposited copper metallisation on various polymers. Electroplating was used to achieve adequate thickness of the metallisation for preparation of adhesion test specimens.

In electroless plating, metal deposition occurs by redox reactions from an aqueous metal salt solution containing a reducing agent. The sample is immersed into the plating bath and the metal ion and reducing agent react on a Pd-catalysed surface. This enables plating on non-conductive surfaces, which is not possible in electroplating. One major advantage of electroless plating is the ability to plate into deep holes and vias. However, deposition rates are generally much lower than for electroplating.[115]

Sputter deposition is one of the physical vapour deposition techniques and nowadays the most commonly used technique in the fabrication of integrated circuits.[116] The process takes place in a low pressure chamber in which an RF field is applied to create a plasma discharge. The ions are accelerated in the field towards the cathode (Cu target). Metallic atoms are ejected from the target and build up layers on any surface they land on. The benefit of RF sputtering is that, because the electrons are oscillating with the RF field, no charge accumulation at the target takes place even if it is an insulator. Hence, RF sputtering is used for the deposition of insulating materials, as well.

Electroplating is a process for metal deposition by electrolysis from an aqueous metal salt solution. In the process, two electrodes, being the sample and a counter electrode, are placed in the plating solution. Deposition occurs only on electrically conductive areas at the sample, which acts as a negatively charged cathode. Current is supplied by an external power supply, and positively charged metal ions migrate to the cathode where they are reduced to metal deposits.[117]

4.1.3 Adhesion tests

The configurations used in the study of interfacial adhesion are presented in Figure 1. The interfacial adhesion of successive polymer layers was studied with configuration B (Publication I), whereas the influence of the configurations on the obtained adhesion strength values was studied with configurations A – D (Publication II). The modified pull-off test that was developed earlier[118] for the study of interfacial adhesion between a polymer substrate and a metal film in miniature structures is shown as configuration E (Publication III-V).

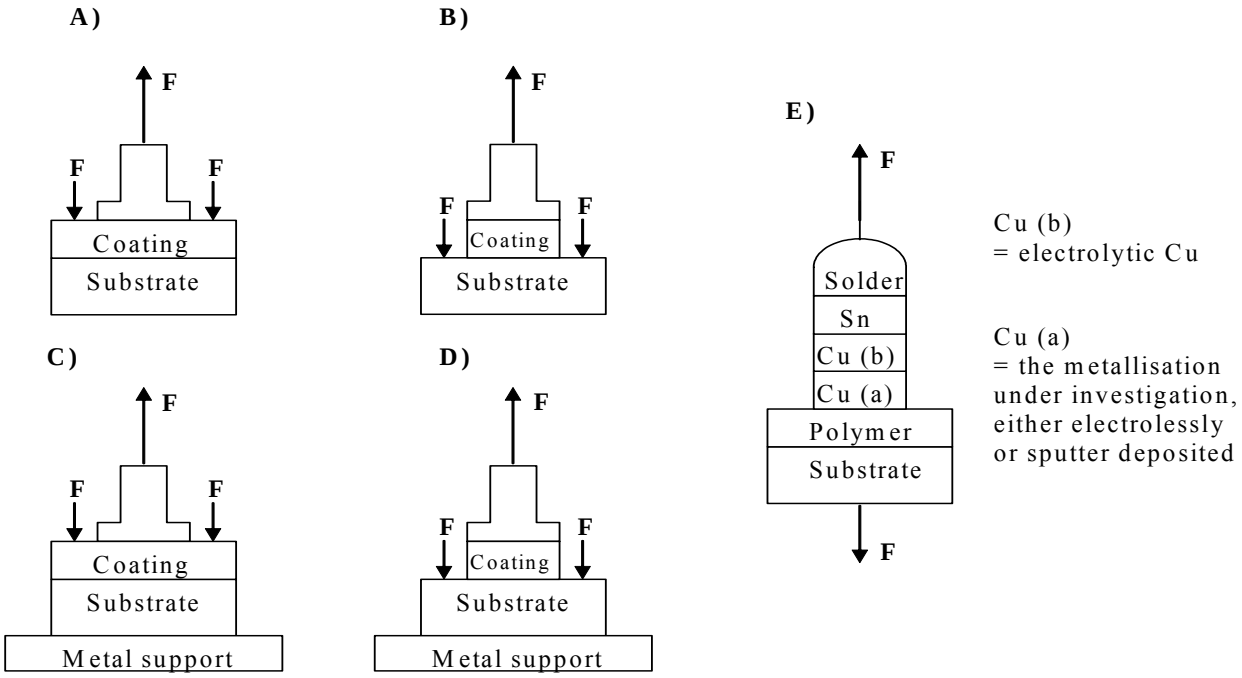

Figure 1. Adhesion test configurations.

4.1.4 Environmental aging procedures

Three test procedures were used to expose the test specimens to environmentally induced stresses. A concise review of the major phenomena resulting in the failure of the polymer/metal interfaces during the environmental testing can be found in Publication II. The first test combined elevated temperature and relative humidity (RH). The test was conducted in a Weiss SB 1180 apparatus according to the IEC 68-2-67 standard at 85±2°C and 85±5% RH for 1000 h. For comparison of the test with a flowing mixed gas (FMG) exposure, the first test was also carried out at 25±2°C and 75±5% RH. The second test, the FMG exposure, was carried out in a Weiss WK1 600 environmental chamber equipped with facilities for controlled dosage of corrosive gases. This test combines the effects of relative humidity (75±5%RH), temperature (25±2°C) and corrosive gases. The IEC-68-2-60 standard (method 4) is applied for 1000 h and makes use of the following corrosive gases: NO_2 (200±20ppb), SO_2 (200±20ppb), H_2S (10±5ppb) and Cl_2 (10±5ppb). Copper sheets and an analysis of the gas concentrations were used to monitor the performance of the test chamber. In a deviation from the standard, the control of the chlorine gas concentration was based on the calculated design value instead of actual measurement. The third test, thermal shock, was carried out in a Weiss TS 130 apparatus for 1000 h (2000 cycles) according to the IEC 68-2-14N standard (+125±2°C/-45±2°C, dwell 15min/15min).

4.1.5 Synthesis of polymer materials

The poly(ε-caprolactone) (PCL) oligomers for blending with SU8 epoxy resin were melt-polymerised from CL at 150°C in a batch reactor under a nitrogen atmosphere utilising continuous stirring. The monomer was fed into the preheated reactor with appropriate amounts of the PGL initiator and $SnOct_2$ catalyst. The reaction time was five hours and the batch sizes were 0.5 kg. After the polymerisation, the hydroxyl end-functionalities of the oligomers were substituted with carboxylic acid in a reaction of hydroxyl group with acid anhydride at 150°C. Reaction time was two hours. Oligomer and an equimolar amount of the anhydride in relation to the hydroxyl groups were fed to the reactor. No catalyst was used in this stage. The reaction schemes of the syntheses are shown in Scheme 1.

A dual-catalysed mixture of the oligomer and epoxy was spin-coated on a substrate at a speed ranging from 1500 to 3000 rpm for 20-60 s. A dual-catalysed mixture was needed to achieve a high degree of crosslinking because an excess amount of epoxy groups in relation to the carboxylic acid

groups of the oligomers was present in the mixture. The crosslinking reactions of the dual-catalysed solution are shown in Scheme 2. In the first bake, the end-functionalised oligomer reacts with epoxy groups. After the first bake, the coatings are exposed to ultraviolet light, which releases the acid-catalyst from the photo initiator. This catalyses the cationic ring-opening crosslinking of the residual epoxy groups during the second bake. The preparation of the coatings was carried out in a clean room (class 1000) to avoid surface contamination.

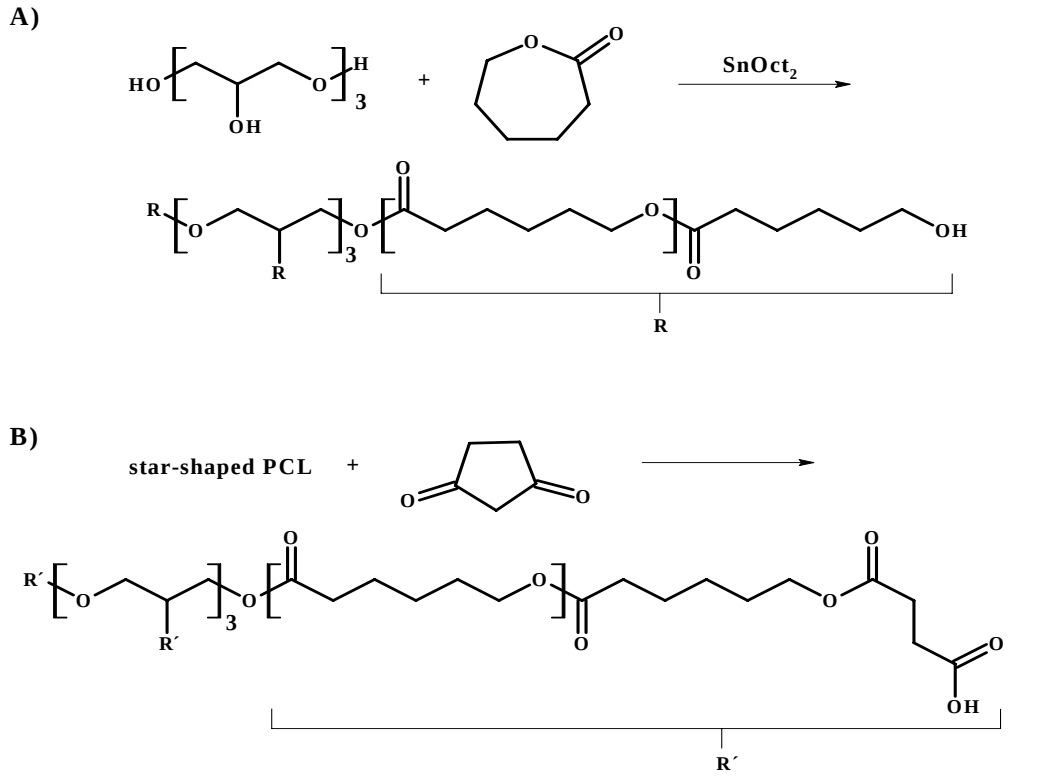

Scheme 1. Synthesis of the network precursor (A) and the substitution of the hydroxyl groups (B).

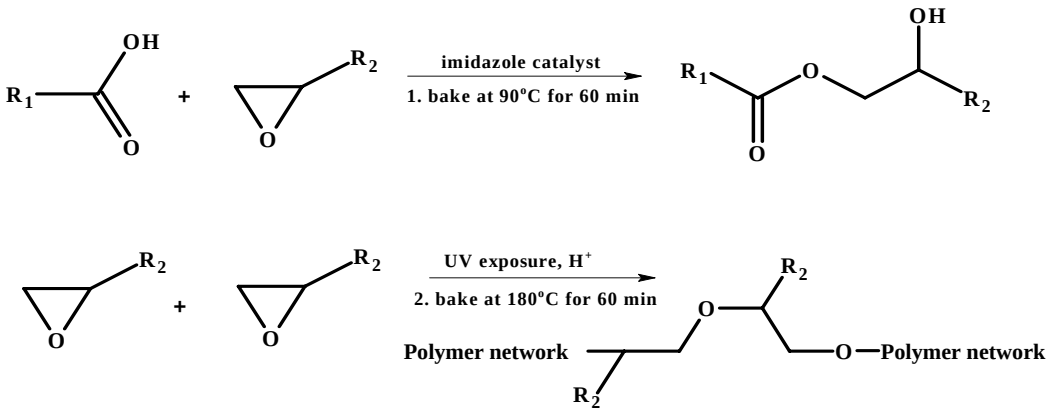

Scheme 2. Reactions of the dual-catalysed crosslinking of 8-functional epoxy with 4-functional oligomers.

4.2 Characterisation methods

The sections below describe in practical detail the most important characterisation methods used in the present work. The methods were used for the investigation of surfaces (4.2.1–4.2.4), adhesion testing (4.2.5), the characterisation of oligomers and crosslinked networks prepared using the oligomers (4.2.6–4.2.10) and the determination of properties of polymeric films (4.2.11–4.2.12).

4.2.1 Scanning electron microscopy and X-ray microanalysis

Scanning electron microscopy (SEM) provides morphological, topographical and elemental information about solid surfaces. The specimen is examined by scanning with a focused electron beam, which interacts with a thin layer of the specimen. This interaction excites several types of emission from the specimen, which can be used to form an image or to obtain elemental information. The appearance of the image depends on the interaction involved and the detector as well as on the signal processing employed. The spatial resolution is limited by the size of the interaction region in the specimen from which the signal is derived and varies considerably, as shown in Figure 2.[119,120] Backscattered electrons can escape from greater depths than secondary electrons and X-rays are produced in an even larger volume and thus have least resolution.

Backscattered and secondary electrons are important in imaging. The origin of backscattered electrons is an elastic scattering of the primary beam electrons by nuclei on the specimen surface. This means that they have almost the same energy as the primary electrons, and significantly more than that of the secondary electrons. The fraction of backscattered electrons escaping at 20 keV varies from 0.06 for carbon to 0.5 for gold.[120] Thus, a backscattered electron image (BEI) exhibits compositional contrast. Because the high-energy backscattered electrons can escape from a larger volume of the specimen than the secondary electrons, resolution is lower at fixed accelerating voltages.

Secondary electrons are produced from the specimen through its interaction with the primary beam. Consequently, the energy of the secondary electrons is decreased relative to that of the primary beam electrons. Moreover, since the secondary electrons can only come from the top few nanometres of the specimen, they are responsible for high-resolution images. A resolution of secondary electron images (SEI) is determined by the beam size (see Figure 2). If the beam falls on a tilted surface or onto an edge, more secondary electrons will escape from the specimen. A feature in the image appears brighter the more secondary electrons are emitted from it. Edges tend to become charged and features extending out from the surface emit more secondary electrons. A

tilted surface enhances secondary electron emission because larger specimen volume interacts with the beam, resulting in increased secondary electron emission. This is shown both schematically and experimentally in Figure 3. Likewise, if the beam falls into a pit or a cavity, fewer secondary electrons can escape because the specimen reabsorbs the electrons.

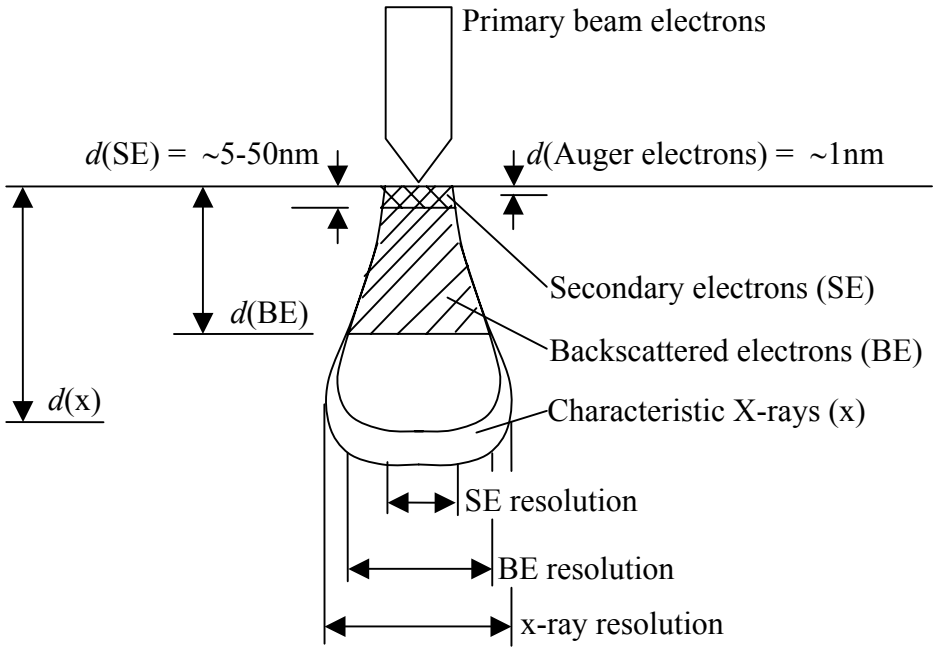

Figure 2. Schematic presentation of the interaction of primary electron beam with a solid surface showing the interaction depth and volume. Redrawn from *Scanning Electron Microscopy and X-ray Microanalysis*.[120]

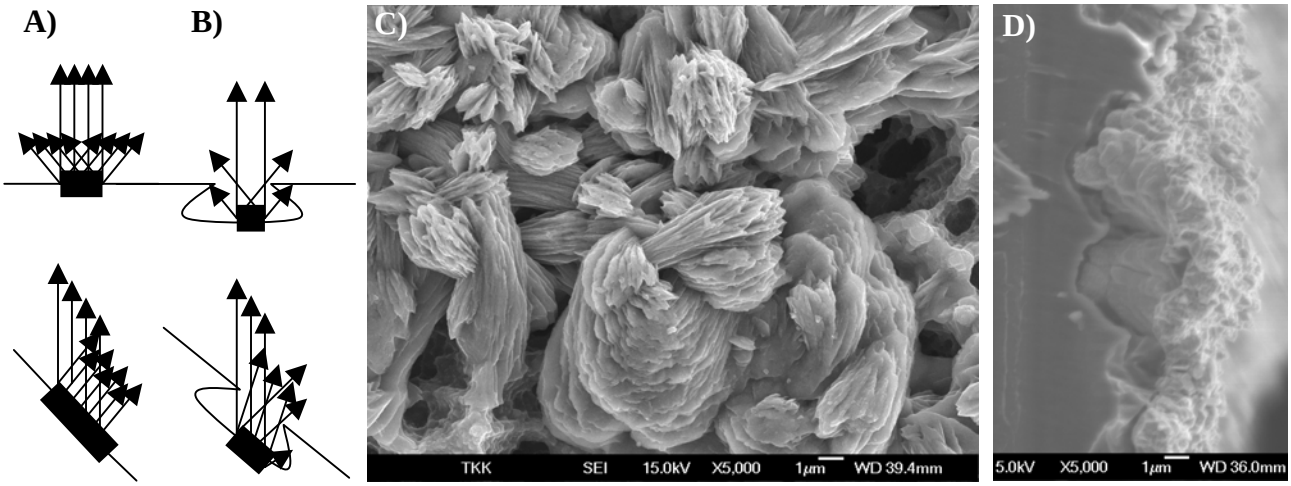

Figure 3. (A) A tilted surface produces more secondary emission because more of the interaction volume is under the electron beam. (B) In a cavity, some secondary electrons will re-enter the specimen and will not be detected. (C) SEI of crystals of a corrosion product on a microporous substrate demonstrating the great depth resolution provided by SEM. (D) Cross-sectional image of a mechanically interlocked electroless copper coating prepared on a microporous surface.

Many polymers are sensitive to the electron beam and exposure can cause artefacts in the image. Mass loss and eventual pitting of the surface and decrease in crystallinity have been observed[120] effects that can change the specimen morphology. The use of low acceleration voltages reduces specimen charging, beam damage and beam penetration, giving greater sensitivity to surface details. Recently, SEM instruments have been improved to give good SEI performance at low voltages (even <1 kV). At low voltage, the resolution of BEI is pretty much the same as that of SEI.[119] Nonconductive materials, such as most polymers, require conductive coatings or the use of very low acceleration voltages to prevent them from charging up in the electron beam. Frequently a thin film coating is sputter-deposited on a polymer sample using carbon, gold or chromium.

The primary beam size is the limiting factor for the resolution. The use of a field emission (FE) source instead of the more regular and cheaper wolfram or LaB_6 filaments allows substantial reduction of the electron beam size and greatly improved resolution. Comparatively high resolution and brightness are maintained at low accelerating voltages in FE-SEM,[121] facilitating the topographical examination of organic samples of both living and synthetic origin. FE-SEM was used to obtain the secondary electron images of surfaces in Publications I-V and VII.

X-rays emitted from the specimen are primarily used for elemental analysis because X-ray radiation comprises well-defined energies characteristic of atoms. A characteristic X-ray emission is the result of the return to ground state of an excited atom. The excited atom is produced by the collision of a primary electron with a core electron of the specimen atom resulting in the ejection of the core electron. The SEM can be equipped with X-ray detectors for elemental analysis. Two types of detectors are used to measure the X-ray intensity, as a function of wavelength or energy. A comparison of energy dispersive X-ray spectrometer (EDS) and wavelength dispersive X-ray spectrometer (WDS) analyses is shown in Table 1. The greatest advantage of SEM X-ray microanalysis over other methods of elemental analysis is that the analysis can be carried out from a comparatively small area (diameter of beam 0.002-0.2 μm). Because X-ray microanalysis is a non-destructive method, the elemental information can be combined with morphology of the specimen. These features make SEM one of the most widely used analytical methods today.

So far, microanalysis has been described as reporting the elemental composition of the very small region of the specimen that interacts with the spot of a focused electron beam. However, it is often more useful to know the concentration of a specific element as a function of its location on the specimen. This is elemental mapping. Instrumentations now available allow simultaneous acquisition of maps for several elements. Digital maps with colours assigned for each element are obtained and permit facile analysis of elemental distribution. This feature was utilised in Publication II.

Table 1. Comparison of EDS and WDS microanalyses.[119]

Energy dispersive X-ray spectrometry	*Wavelength dispersive X-ray spectrometry*
Simultaneous detection of elements	Quantitative analysis of one element at a time
Rapid analysis (~100 s)	Slow analysis (from 5 minutes to hours)
Spatial resolution a few micrometres	Spatial resolution 1-5 micrometres
Background counts from backscattered electrons reduce sensitivity	Peak/background ratio 10 to 50 times better than EDS, good sensitivity
Serious peak overlap problems	Good energy resolution, little peak overlap
Single detector	Several detectors needed to cover a range of elements
Detection limit Z>5	Detection limit Z>3

4.2.2 Atomic force microscopy

Scanning probe microscopy (SPM) is the general name for the variety of microscopes that have one basic thing in common: the image is obtained by scanning with a solid probe on or just above the surface of a specimen to detect a signal from the interaction of the probe with the surface. The resolution of the image in SPM is limited to the region of interaction, and therefore the probe is constructed with a very fine tip. Several forms of SPM provide resolution at the atomic level.[119] The first SPM to be developed was the scanning tunnelling microscope (STM) where the probe is a conductor set at a small bias voltage difference from a conducting sample, and the signal is a current that passes between them.[122] However, non-conducting samples had to be coated with a thin film of conductive material, which is likely to affect the fine structure detail in nanometre scale. The study of non-conducting materials was greatly improved by the development of atomic force microscopy (AFM).[123] The atomic force microscope is often called a scanning force microscope as a more general term for all kinds of probe microscopes relying on the measurement of frictional, hydrophilic, magnetic, and acoustic forces. Atomic force microscopy is currently the most important form of SPM for the study of polymers because there is no need for the sample to be conductive.[124]

Despite the benefits of AFM, it cannot replace traditional electron microscopy. Rather, AFM must be regarded as a complementary technique. In addition, the study of soft polymeric materials by AFM requires that great care betaken to avoid artefacts. Substantial alteration and damage (sample dragging) appears on soft organic materials during scanning in the contact mode, as well as

severe loss of probe quality (dull tip and multi-tip effects).[119] To solve these problems, the so-called tapping mode has been devised, in which the tip oscillates (frequencies 50-500 kHz) at tip amplitude of about several tens of nanometres.[125] Since the tip is no longer in permanent contact with the surface during the scanning motion, the tip is prevented from sticking to the surface and is not pulled sideways by shear or frictional forces.[124] This mode of operation is used in Publications I, III-V. Reliable and reproducible operation of tapping mode AFM enables lateral resolution of the order of a few nanometres and vertical resolution less than 1 Å.[119,124]

A combination of AFM and SEM provides valuable information for topographical studies of roughened surfaces. AFM can provide a quantitative value for the roughness, but it does not always reveal the nature of the roughness (wavy, needles, spheres, cavities), which in turn can be obtained from SEM investigation. Information about the parts that the probe of the AFM never contacts, i.e. the cavities of porous surface, cannot, of course, be recovered. SEM can provide an impression of three-dimensionality to a topographical image better than any other microscope. The examination of porous surfaces, in particular, benefits from the combined use of SEM and AFM, as is shown in Figure 4 for the surface of a heterogeneous photodefinable epoxy modified by wet-chemical method.

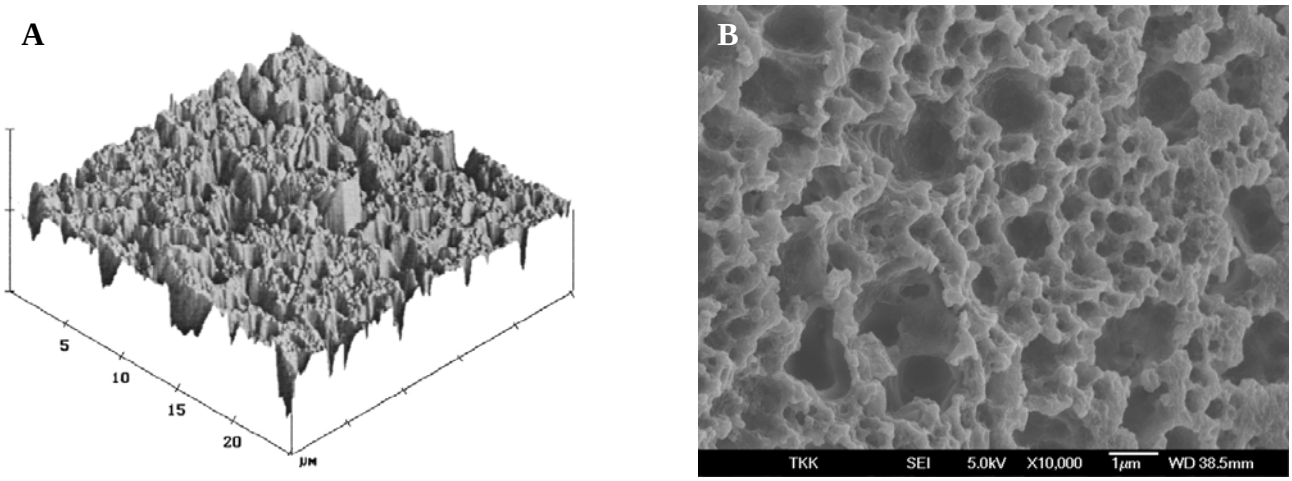

Figure 4. Comparison of images obtained by a) AFM[126] and b) SEM (specimen tilted at 45°) from Probelec 81/7081 surface roughened by wet-chemical method. Figure 4a is reproduced by permission of The Electrochemical Society, Inc. Siau S., Vervaet A., Schacht E., van Calster A., Influence of chemical pretreatment of epoxy polymers on the adhesion strength of electrochemically deposited Cu for use in electronic interconnections, J. Electrochem. Soc., 151, C133 (2004).

4.2.3 X-ray photoelectron spectroscopy

X-ray photoelectron spectroscopy (XPS) is used to obtain information about the elemental composition and the oxidation state of the elements being examined. Often the surface composition of a solid differs, at least to some degree, from the bulk composition. The high surface sensitivity provided by XPS is the greatest asset of the method in comparison with other surface analytical methods. Photoelectrons are produced in the interaction of a probe with a specimen and the probe in XPS is an X-ray beam. The use of a low atomic number X-ray source (typically Mg or Al) employing a crystal monochromator allows narrow bandwidth of the K_α lines (0.3 eV), which in turn enhances resolution, enables a smaller spot to be probed, and decreases background emission. Attenuation of the emitted electrons is avoided by carrying out the examination under a pressure of 10^{-3} Pa. Often, even better vacuum (10^{-7} to 10^{-8} Pa) is required to deadsorb oxygen and water from the specimen.

The sampling depth, d, in XPS is described by $d = 3\lambda\sin\theta_t$, where λ is the inelastic mean free path (IMFP) for photoelectrons and θ_t is the take off angle for photoelectrons with respect to the sample surface. The IMFP is the average distance that an electron with a given energy travels between successive inelastic collisions. The constant 3 comes from the intensity attenuation according to Equation 3:

$$I_d = I_0 e^{-(d/\lambda)} \qquad 3$$

where I_d is the intensity of a given photoelectron that has escaped from the specimen surface and I_0 is the intensity of a given photoelectron at depth d. When d equals 3λ the intensity ratio I_d/I_0 is 0.05, according to which 95% of the detected photoelectrons must come from the sampling depth. The IMFP is a function of the kinetic energy (E_k) of the emitted photoelectron and the material. E_k is a function of the X-ray source employed. For polymers containing aromatic groups, λ obtains values around 3 nm.[127-129] The influence of take off angle (θ_t) on the sampling depth is shown in Figure 5.

The sampling depth is maximised at 90° take off angle. In the analysis of microscale roughened surfaces, the use of $\theta_t < 90°$ allows an analysis of the peaks only because the sampling depth in polymers is less than 10 nm and thus part of the emitted photoelectrons are attenuated into the cavity walls of the "tilted" specimen. The angle of incidence (θ') has no significant effect on the outcome of the analysis because the X-ray penetrates relatively deep into the specimen, but the

sampling depth is limited by the escaping photoelectrons. Usually the angles of incidence and take off cannot be adjusted independently.[64]

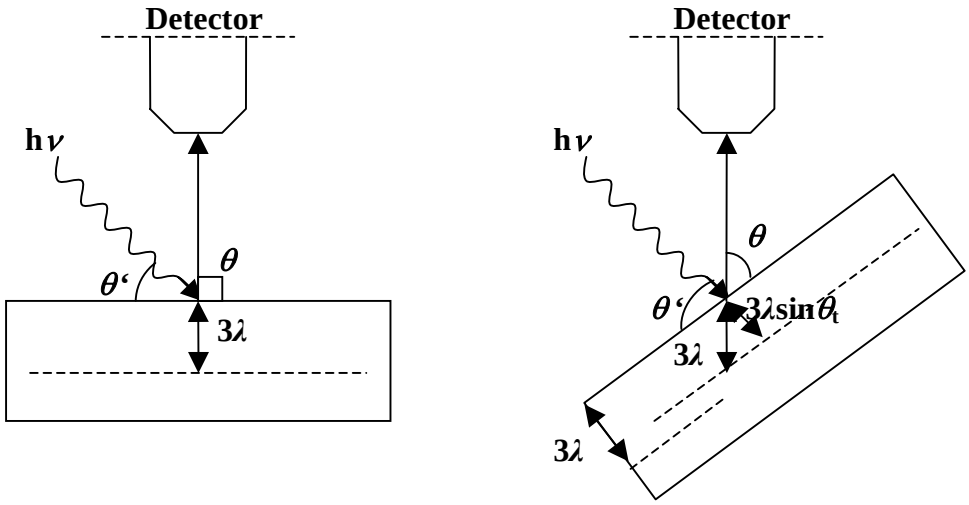

Figure 5. Effect of take off angle on the sampling depth.

The XPS analysis is based on the measurement of the kinetic energy (E_k) of the emitted electron with a spectrometer. The binding energy of the electron, E_b, can be calculated from Equation 4

$$E_b = h\upsilon - E_k - w \tag{4}$$

where w is the so-called work function of the spectrometer and $h\upsilon$ is the energy provided by the X-ray beam. The binding energy of an electron is characteristic of the atom and orbital from which the electron is emitted. E_b increases with the atomic number of the element. Qualitative elemental composition of the specimen is determined from a low-resolution spectrum sometimes called a survey or overall spectrum. This spectrum is obtained using E_k in the range 250-1500 eV, which correlates with binding energies in the range 0-1250 eV. All elements are detected except hydrogen and helium, providing that the specimen contains more than 0.1% of the element.

The position of the binding energy peak also depends in some degree on the chemical environment of the atom responsible for the peak. These so-called chemical shifts can be differentiated under the conditions of a high-resolution examination. A high-resolution study thus enables detection of the chemical bonds. The greater the ability of the neighbouring atom to withdraw electron density from the atom under investigation, the higher the effective nuclear charge

of the atom and, as a consequence, the higher the binding energy is. Chemical bonds can be identified by applying curve-fitting routines to the peaks obtained from the high-resolution study. The curve fitting and background subtraction procedures are explained in more detail in Publication II. Quantitative information about the elemental and chemical bond proportions is obtained by integrating the areas of the identified peaks. High-resolution XPS was used in Publications II-V to follow the effects of the surface treatment on the surface chemistry. One of the most important applications of XPS has been identification of the oxidation states of elements present in inorganic matter. XPS was applied in this way to determine the oxidation state of copper after an oxidative treatment, as reported in Publication II.

4.2.4 Contact angle measurements

A liquid forms a sessile drop on a solid surface, which is easy to visualise and enables measurement of the contact angle. The contact angle is simply the angle between the surface and a line that is tangent to a drop of liquid on the surface at the point where it intersects the surface, as shown in Figure 6. But, the quantity on which Young's equation is based, namely the measurement of the equilibrium contact angle (θ_e), is not always easy. In fact, the value of the experimentally obtainable contact angle is not unique for each system; at least two values are commonly measured–the advancing and the receding contact angles. The advancing contact angle was used in this work because it best represents the equilibrium state.[67]

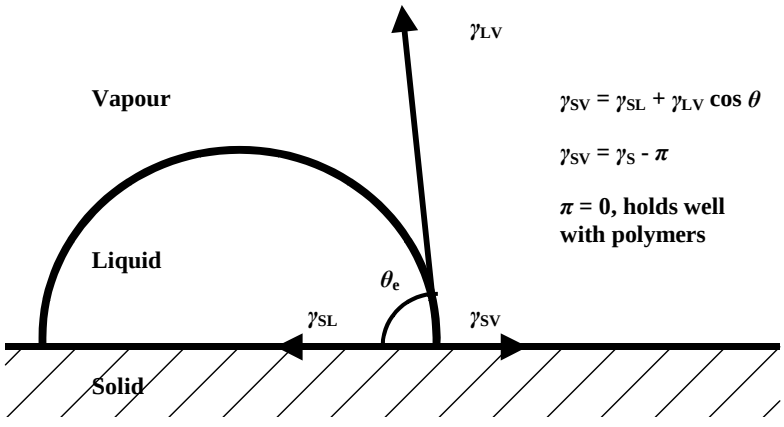

Figure 6. Sessile drop at equilibrium with a solid surface and the saturated vapour of the liquid. The surface free energies are tied together with Young's equation. π is spreading pressure, and it is considered negligible in the case of polymers, yielding γ_s to represent the surface free energy of the solid in air.

Two approaches are used to measure contact angles: tensiometry and goniometry. Tensiometry involves measuring the forces of interaction when a solid is contacted with a probing liquid. Goniometry involves the observation of the drop of a probing liquid on the solid surface. Goniometry was selected for this study because it is more versatile, and the sample preparation is easier for sessile drop observation than for tensiometry. The main elements of the goniometer include a light source, sample holder, microsyringe, image capture, and software for analysis of the drop shape and contact angle. A drop with either advanced or receded edge is produced with the microsyringe. An advancing contact angle is produced by introducing the probing liquid on the surface, whereas a receding angle is produced by withdrawing a sufficient amount of liquid from a drop resting on a solid surface. Measurements of contact angle were used to follow changes in the surface free energy of polymeric materials and the hydrophilicity or hydrophobicity as a function of various surface treatments (Publications I, III-V and VI).

4.2.5 Pull-off test

The pull-off test is a simple method to measure interfacial adhesion. In an ideal case it resembles a tensile test, which is described later, and provides the fracture strength of the weakest interface/phase. Careful execution of the test is mandatory, however, to obtain reliable and meaningful results that are of use in the improvement of the polymer-based interfacial structures found in electronics. The procedures used to prepare adhesion test samples for the examination of epoxy adhesion to copper, and *vice versa,* are presented in detail in Publications II and V, respectively. Applications of the pull-off method are described in Publications I-V. Publication I reports an evaluation of the interfacial adhesion of successive epoxy coatings. Publication II focuses on the evaluation of the pull-off method itself and points out the effect of environmental stresses on the durability of interfacial adhesion between copper substrate and epoxy coating. Publications III-V report the use of a modified pull-off test to study the adhesion of deposited copper to differently treated surfaces of various polymer substrates.

4.2.6 ^{1}H and ^{13}C Nuclear magnetic resonance spectroscopy

Nuclear magnetic resonance (NMR) spectroscopy makes possible the direct observation of atoms. Both solution and solid-state NMR techniques are available. Here the principle of solution NMR spectroscopy of polymers is briefly described. The main part of the NMR instrumentation is a

strong magnet that provides an external magnetic field (B_0). When an atomic nucleus (which is positively charged) spins, it generates an electric current, which has a magnetic moment (μ) associated with it. Two processes take place when spinning nuclei are placed in the external magnetic field. First, the nuclei start precession about the axis of B_0. Second, the spinning nuclei, providing that they possess a nuclear spin quantum number (I_n) ½ or 1, thus being magnetically active, become oriented. The nuclei with $I_n = 1$ have three allowed ($2I_n + 1$) spin states (I_Z = 1, 0 and -1), and nuclei with I_n = ½ have only two (I_Z = ½ and -½), as shown in Figure 7(a). These states are not energetically equal. In the low-energy state the magnetic moment of the nucleus is aligned with (I_Z = ½) the external magnetic field and in the high-energy state it is against (I_Z = -½) the field. The two spin states coexist, but because the parallel orientation is favoured it is slightly more populated than the antiparallel. This excess results in a net magnetic moment $\overline{M}$ aligned with the B_0 as shown in Figure 7(b). Nuclei having I_n equal to zero do not possess angular momentum in any external magnetic field and thus cannot exhibit nuclear magnetic resonance.

NMR spectroscopy arises from the use of nuclei that have spin quantum number ½. When the oriented nuclei are subjected to very brief pulses of suitable radio frequency (RF) (B_1), they absorb a quantum of energy. The magnetic moments of the nuclei are forced to bend toward the xy-plane and eventually the net magnetisation vector precession commences around B_1. The nuclei are then in resonance with the applied radiation. Simultaneously an RF current is induced in a coil along the y-axis and this is taken as the NMR signal. The events taking place during the irradiation are shown in Figure 7(c-f).

The frequency at which the NMR signal appears depends mainly on the strength of the external magnetic field. At 7.04 Tesla, for example, protons resonate with a frequency of 300.03 MHz. The chemical environment of an active nucleus, however, causes a small shift in the resonance frequency–the chemical shift–at the range of ppm deviation off the intrinsic resonance frequency of the given atom. By sweeping the frequency, and hence the energy of the pulsed electromagnetic radiation (B_1), a plot of frequency versus energy absorption can be generated. This is the NMR spectrum. The intensity of the signal provides quantitative information about the proportion of the chemically different nuclei of interest in the sample. One type of nucleus is observed at a time. An atomic nucleus has I_n = ½ only when the number of one of the nucleons–proton or neutron–is odd, while the other is even. Such nuclei include ^{1}H, ^{13}C, ^{15}N, ^{19}F, ^{29}Si and ^{31}P. Of these ^{1}H (99.98%) is a very common isotope in nature, while ^{13}C is rare (1.11%). The rarity causes practical problems in sample preparation, and the acquisition time of a ^{13}C NMR spectrum is long in comparison with the ^{1}H NMR spectrum. In addition, the proton nucleus has a simpler

magnetic field than the ^{13}C nucleus and the sensitivity of proton analysis is thus better. Small molecules give a highly accurate proton spectrum, but the analysis of large molecules such as polymers results in broad signals because of the random-coil structure that the molecules assume in solvent. In polymer analysis, therefore, it is occasionally necessary to use ^{13}C NMR analysis instead of proton.[130-132] ^{1}H and ^{13}C NMR analyses were used in studies described in Publications I, VI and VII to verify the structure of network precursors. The interpretation of the spectra of oligomers is explained in more detail in Publications VI and VII.

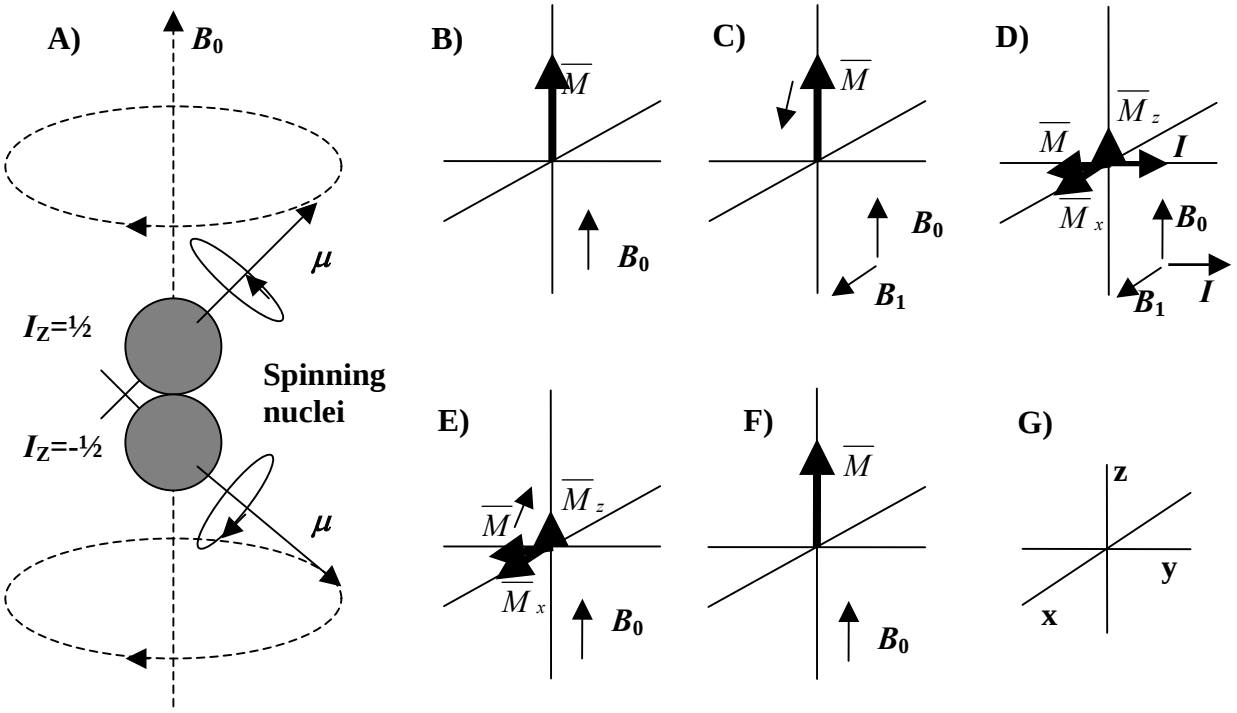

Figure 7. Precession of rotating nuclei, having a I_n = ½, in the B_0 (A) and the resulting $\overline{M}$ (B). The external RF pulse (B_1) bends the $\overline{M}$ in the case of resonance (C), while the amplitude and applied pulse time determine the resulting angle between B_0 and $\overline{M}$. Once the pulse is shut down, the relaxation of $\overline{M}$ starts (E-F). Labelling of the axes is given in a different presentation (G) for purposes of clarity. Note: The RF receiver is a coil prepared around the y-axis to which the current (I) is induced from $\overline{M}_x$ during the pulse and taken as the NMR signal.

4.2.7 Fourier transform infrared spectroscopy

Fourier transform infrared (FTIR) spectroscopy provides information about the functional groups of an organic molecule and is a valuable complementary method for NMR spectroscopy in the elucidation of molecular structure. Functional groups found in polymers include hydroxyl, carboxyl, ester, double bond, epoxy, phenol and aromatic ring. The application of electromagnetic radiation in

the infrared region, λ = 2.5–50 μm, results in interaction with the covalent bonds of the molecule. The FTIR spectrum shows either the absorption or the transmittance of light in percentage as a function of wavelength (λ) or often as its inverse, i.e. the wave number.

The molecule interacts with electromagnetic radiation, the interaction depending on the existence of an electric moment across the bond under consideration. Before it can exhibit infrared absorbance, a molecule must include polar bonds, though not necessarily permanent dipole moments. Quantitatively, the amount of energy absorbed at a given frequency depends on both molecular concentration and molecular structure.[131-133] The possible interactions are shown in Figure 8. FTIR spectroscopy was used to identify functional groups in the oligomers and networks studied in Publications I and VI.

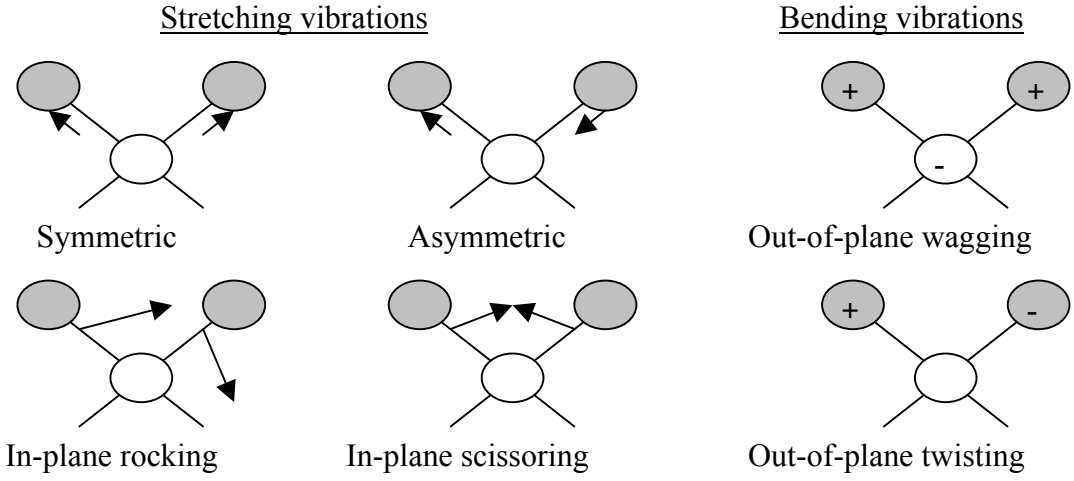

Figure 8. Types of molecular vibrations. Note: + indicates motion from the plane of the paper towards the reader and– indicates motion away from the reader.

4.2.8 Size exclusion chromatography

Size exclusion chromatography (SEC) is used to determine the molecular weight of large molecules. It is a proportional method and does not yield absolute value. The heart of the SEC instrument is a set of columns connected in series and packed with porous beads. Analyte molecules in a diluted solution diffuse into the pores as the solution is pumped through the columns at a constant rate. Usually four columns are connected in series and each of them is packed with beads of different pore size. The average pore size ranges from 100 to 10^5 Å. The average residence time of the analyte molecule in the pores depends upon the effective size of the molecule. The results are thus provided in the form of signal intensity as a function of retention time. The interaction between

the beads and the solution is minimised. Molecules larger than the pore size of the beads are excluded and suffer essentially no retention. This means that the larger molecules are the first to be eluted and detected by the optical detector at the end of the column system. Molecules of significantly smaller size than the pores permeate throughout the pore labyrinth, entrapping into the pores for the greatest time. Between these two extremes are intermediate size analyte molecules whose average retention time in the columns depends linearly upon their diameter and only to some extent on molecular shape. Hence, the calibration is done with use of linear polystyrene standards of known molecular weight. However, highly branched molecules can assume significantly different shape in relation to the random-coil structure that most linear polymers assume in the solvent.[133,134] SEC was used only as a qualitative tool, therefore, to check peak shape and size of the star-shaped oligomers, as reported in Publications VI and VII. The broadness of the peak provides information about the molecular weight distribution (MWD) and the appearance of multiple peaks indicates that there are molecules of distinctly different size.

4.2.9 Differential scanning calorimetry

Differential scanning calorimetry (DSC) is the most widely used method in the thermal characterisation of polymeric materials. In addition, DSC provides a means to measure the heat of various reactions (ΔH_r), which can be used to deduce conversion and, in particular, to evaluate reaction kinetics. Two approaches are used to obtain DSC data:[53,135] a power compensated DSC and a heat flux DSC. Here the heat flux was used. The heat flux DSC measures differences in heat flow into a sample and a reference as a function of sample temperature while the two are subjected to a controlled temperature–time program. DSC was used in studies described in Publications VI and VII for the thermal characterisation of oligomers and for the evaluation of reaction kinetics. The principle of model-free kinetic evaluation is presented in section 4.3.3.

4.2.10 Mechanical testing

The mechanical properties determine the range of usefulness of a material and establish the service that can be expected. The mechanical properties can be represented by a stress–strain diagram. A fundamental method for the determination of stress–strain behaviour of materials is tensile testing.

In tensile tests, a carefully prepared specimen with a known cross-sectional area is clamped between a moving crosshead and a load cell. The crosshead allows for a predetermined displacement or loading rate. The load cell senses the force developed in the specimen as it

elongates, and the output of the load cell is recorded. From the data, a curve of load as a function of displacement is generated, which is then converted to an engineering stress–strain curve by dividing the load by the original cross-sectional area of the specimen, and dividing the displacement by the original gauge length.

When a load applied to a specimen in a tensile test causes a stress that remains below the yield stress of the given material of the specimen, the deformation is said to be elastic and the strain thus induced is completely removable upon elimination of the load. Stresses equal to or greater than the yield stress of a material result in a plastic deformation, which means that the deformation is no longer recoverable. Any stress above the yield stress is referred to as a flow stress. The ratio of elastic to plastic deformation provides information about a material's ductility. The total strain (ε) can be broken down into elastic strain (ε_e), plastic strain (ε_p) and strain at fracture (ε_f). The tensile strength (δ) is the maximum stress that the specimen can undergo in the test. The elastic modulus (E) is obtained from the slope of the stress–strain diagram in an elastic zone where the relation $E = \delta/\varepsilon_e$ holds. Toughness (G) can be considered to represent the measure of work needed to achieve the fracture; it is obtained, therefore, from the area between the stress–strain curve and the strain axis.[136,137]

In real situations, materials are always under multiaxial loading. Several tensile and shear stress components are thus acting on the specimen at the same time. In addition, the mechanical properties of materials are highly strain rate dependent. Some ductile polymers, for example, may behave like brittle materials at high strain rates. Mechanical properties are, of course, dependent on temperature, and dynamic mechanical analysis is a suitable method for the study of thermomechanical properties.

The flexural or three-point bending test is somewhat more complex than the tensile test because the distribution of the stress on the sample during the test is non-uniform. In the three-point bending test, the specimen is placed on two supports and a bending force is applied in between the supports from above. The three-point bending test provides information about the specimen's stiffness, and if the specimen is broken in the test it yields flexural strength. If the specimen is pre-cracked, this same test mode can be used to determine the fracture toughness (G_c).[136,137] Mechanical properties of selected oligomer networks are reported in Publication VI.

4.2.11 Dynamic mechanical analysis

Dynamic mechanical analysis (DMA) provides information about a material's time and/or temperature dependent modules and energy-dissipative mechanisms. The use of DMA in polymer

characterisation has proven to be extremely useful in identifying the major molecular relaxation at T_g as well as secondary relaxations below T_g. The T_g is attributed to the relaxation of the amorphous domain of the material and the secondary relaxations are associated with the motions of specific structural units such as the rotation of side chains and the movement of functional groups within the polymer molecule.[136,138]

In the DMA instrument, the specimen is exposed to a forced vibration and the response of the material is followed. The extent of damping to which the cyclic strain lags behind the applied stress wave is measured. The use of oscillating force enables the differentiation of the material response to elastic and plastic components. The elastic modulus is the part of the applied stress that is in phase with the oscillation and for this reason is called the storage modulus, whereas the loss modulus represents the part of the applied stress that is out of phase with the oscillation and is completely dissipated (mostly in the form of heat). Often the frequency is set at 1 Hz and the experiment is conducted over a range of temperatures. This results in the presentation of responding force as a function of temperature, which is then converted to a stress/temperature diagram.[136,138] Many test configurations are possible, including torsion, tension and three-point bending, of which the last was used in the study of Publication VII to obtain information about both temperature dependent response and the ductility of reactively blended epoxies.

4.2.12 Spectrophotometry

Determination of refractive index

The use of two-angle spectrophotometry to determine the refractive index is well established; the details of the measurement procedure can be found in reference 134. Briefly, the reflectance spectrum is collected from normal and 70° angles of incidence and the absolute reflectance spectrum is obtained by comparing the sample data with a previously measured reference spectrum. We used a silicon wafer as the reference, which has well-known optical characteristics. In addition to a reference, the determination of optical constants demands material modelling software, which is used to generate a simulated reflectance spectrum based on a predetermined layer structure and material models.[139] The material models are dispersion formulas capable of describing the variation in the refractive index of the material as a function of the wavelength within the measured wavelength range.[139] In the current work, the Cauchy model[140,141] was used as dispersion model for the polymeric films. A regression on the unknown model parameters was then performed to minimise the error function of the experimental and simulated reflectance spectra.

Determination of film thickness

The wavelengths at which maximum reflectance appears in the reflectance spectrum can be obtained from Equation 5,

$$\lambda(\max) = \frac{2nd\cos(\phi')}{m} \tag{5}$$

where m = 1, 2, 3, …, n is the refractive index of the film, d is the thickness of the film and ϕ' is the angle between the normal of the film and the ray of the reflected light in the film. By taking two measured wavelengths, both at maximum reflectance, and subtracting one from the other using Equation 5, one gets Equation 6 for the film thickness (d),

$$d = \frac{i\lambda_0\lambda_i}{2n(\lambda_i - \lambda_0)\cos(\phi')} \tag{6}$$

where i = the number of complete cycles from λ_0 to λ_i, the two wavelength peaks that define the i cycles. For two adjacent maxima the i is 1. If the refractive index n is known, the determination of thickness d is straightforward.[142] In the present study, however, a new material was characterised and for the simultaneous determination of n and d, the dispersion formulas given above had to be employed.[140,141] Because two angles are measured simultaneously, the film thickness and refractive index can be determined independently.[139]

Method to determine thermal properties

Calorimetry is the preferred measurement technique for glass transition studies of materials since it yields values for thermodynamic properties. Unfortunately, conventional differential scanning calorimetry (DSC) systems are of limited use for studies on thin films. The sample size is so small that the required level of sensitivity for the measurement is usually beyond the limits of conventional DSC instruments.[53] A variety of other methods for measuring the T_g of thin films have been reported in the literature, among them ellipsometry,[143,144] X-ray reflectivity,[58,145,146] interferometry,[147] Brillouin light scattering[57] and positron annihilation[148]. A non-destructive method that would allow simultaneous characterisation of the optical and thermal properties of films in the often encountered thickness range of a few micrometres thus appeared extremely attractive.

A novel way of utilising spectrophotometry data is to use it to determine a glass transition temperature (T_g) and the out-of-plane coefficient of thermal expansion for supported polymeric films. To do this, a heating chuck was employed, which enabled the determination of the temperature (T) dependence of the film thickness (d) and the index of refraction (n). The T_g and the out-of-plane coefficient of thermal expansion (CTE) of a polymer film were determined from the obtained thermal dependence of the refractive index and film thickness, respectively. We collected the data with a FilmTek 4000 fibre-optic based spectrophotometer from Scientific Computing International with a temperature range of 25–200°C and heating rate of 1°C/min.

It was assumed that the T_g of a film would appear as a change in the slope of the n-T and t-T curve.[149] A Matlab® code was written to enable automatic calculation of the point of change in the slope. The program divided the curve into two parts at each temperature interval and performed a linear fit for both parts. The residuals were collected to determine the error of the fit. Temperatures were scanned and the sum of the residuals was calculated at each point of temperature. The point at which the change in slope appeared was then taken to represent the glass transition temperature of the film. The point itself was the minimised sum of the residuals of the linear fit. The coefficient of out-of-plane thermal expansion (CTE) for the films was calculated both below and above the T_g on the basis of the temperature dependence of the film thickness.

4.3 Evaluation methods

The sections below describe briefly the backgrounds of the evaluations methods utilised in the present work to obtain essential information of surfaces (4.3.1), the employed adhesion test (4.3.2) and reaction kinetics (4.3.3).

4.3.1 Evaluation of solid surface free energy

Direct measurement of solid surface free energy is impossible except in special circumstances in which the molecules of the solid have some mobility, as, for example, in metals at temperatures close to their melting points.[69] A few indirect methods are presented in the literature, including but probably not limited to the use of atomic force microscopy,[150] gas chromatography[151] and contact angle measurements.[69] The surface tension of simple fluids can be calculated fairly accurately and surface properties of crystals can be estimated theoretically.[67,69,152-154] Although significant progress has been made in the attempt to calculate surface free energies at 0 K, the calculation approach is unlikely to be of practical importance in the foreseeable future. This is because of the difficulty in

calculating high temperature thermodynamic properties with the required accuracy even for binary alloys, not to mention heterogeneous polymers.[155] In addition, during the crosslinking of a thermosetting polymer its chemistry is changed radically and irreversibly. Indeed, this was demonstrated in Publication I.

Because of the fundamental limitations of the calculation and direct measurement of surface free energy of thermosetting polymers, semi-empirical approaches were employed here. By far the most widely used method is to evaluate the surface free energy of a solid from its contact angles with one or more liquids of known surface tension.[156-167] However, the surface science community is still discussing the correct way to measure contact angles[168] and to evaluate the surface free energy of solids.[166,167] All these subjects are of increasing practical importance, but many fundamental discoveries have yet to be made. As long as no method for the determination of real surface free energy quantities is available, however, even relative values charged with many simplified assumptions will be useful in achieving better understanding of the wetting processes.

Contact angles are a measurable manifestation of the surface free energy, which in turn determines the wetting of materials. For a drop to spread on a surface, its surface tension must be less than the surface free energy of solid. Therefore, the determination of solid surface free energy of solids is important. At present, the approaches of practical importance and by far the most cited models to evaluate solid surface free energy are based on Young's equation (Eq. 7), which demands the measurement of contact angles.

$$\gamma_{lv} \cos\theta = \gamma_{sv} - \gamma_{sl} \tag{7}$$

The known parameters in Young's equation are the surface tension of liquid, γ_{lv}, and the contact angle, θ, and it is assumed that the solid–vapour surface free energy (γ_{sv}) can be provided by this equation. However, the solid–liquid surface free energy (γ_{sl}) is unknown. If this parameter could be expressed by another equation in terms of γ_{lv} and γ_{sv} the problem could be solved.

Three basic approaches have been taken to solve the problem just mentioned. The first approach seeks to find a mathematical relationship for γ_{sl} in terms of γ_{lv} and γ_{sv} and then evaluate the unknown γ_{sv}. This approach has led to the formulation of several "equation-of-state" models, the latest modification of which has been presented very recently.[156] The second approach approximates the surface free energy of a solid by using the concept of critical contact angle.[157] The models based on this approach assume that the surface tension of a liquid that exhibits zero contact angle on the solid surface is equal to γ_{sv}. These models generally yield values lower than the models

based on the other two approaches, however, and require the use of many homologous probing liquids, which is time-consuming.[158] Because of these drawbacks the second group of models was not considered in this study. The approaches belonging to the third group were originally developed to provide an explanation for results obtained working within the context of the critical surface angle described above.[157] These approaches divide the surface free energy into dispersion, polar and acid-base components.[159,160] The γ_{sl} is then expressed in terms of the components of γ_{lv} and γ_{sv}. Models formulated according to this approach include geometric mean,[161,162] harmonic mean[158] and acid-base[163-165] models, and the determination of γ_{sv} by these models requires a measurement of contact angles of two to three liquids on a given solid with known components of the surface tension. Models one and three are discussed in Publication I and all three models in references 156-167.

4.3.2 Modelling of adhesion test set-up using a finite element method

A finite element method (FEM) divides a problem domain into a collection of sub-domains (elements) of significantly small size and standard shapes (triangle, tetrahedral etc.) with a fixed number of nodes at the corners of the given shape. When a linear square element is used, four nodes define the element. FEM calculations are based on the imposed boundary conditions and on the inserted parameters of the materials such as the modulus of elasticity (E) and Poisson's ratio (v). Here, the material behaviour was assumed to be elastic for all the materials present in the test set-up and only the values for E and v were inserted. As the boundary condition, either displacement or force is given for each node. Linear elastic theory approximations representing the behaviour of the material are done using polynomial functions within each element to generate a local solution. The linear elastic theory is assumed to be valid for highly crosslinked epoxy in the glassy state. In fact, the materials, especially epoxy, do not behave in completely elastic manner, but after thoughtful consideration it was concluded that an elastic model would reveal the studied stress distribution with adequate accuracy. Moreover, utilising a linear elastic model instead of a viscoelastic model for the polymer saves considerable calculation time. Tying together the local elemental solutions yields a global system whose solution produces the model of an existing stress distribution in the problem domain.

FEM calculations were used in Publication II to determine the stress distribution in the vicinity of interfaces of materials of interest in the interfacial adhesion tests. Various adhesion test configurations were studied to obtain better understanding of the test and to improve it on the basis of the modelling outcome. Knowledge of the stress distribution in a test specimen helps in

interpreting the interfacial adhesion results and, in particular, provides essential information about the validity of a given test configuration.

4.3.3 Model-free evaluation of crosslinking kinetics

The study of reaction rates and their dependence on temperature provides essential information about the practical and fundamental aspects of reactions. This information can be obtained by various methods including thermogravimetry and differential scanning calorimetry (DSC). The reason why DSC is so widely used is that most phase transitions, be they melting, glass transformation or chemical reactions, are accompanied by a change in heat. While the kinetic analysis of simple reactions on the basis of DSC data is well established, Galwey,[135] at least, notes that he is "distinctly disappointed" by the lack of proper methods for the study of complex reactions.

At the moment, a model-free kinetic approach provides a route to obtain useful information, although not complete understanding of the reaction kinetics of multi-step reactions. With very few exceptions the rate of a reaction increases with the temperature. The relation between rate constant, k, and temperature, T, was first proposed by Arrhenius:

$$k = Ae^{-E/RT}. \tag{8}$$

The constant A is called the pre-exponential factor, E is the activation energy and R is the gas constant. Kinetic analysis of an epoxy crosslinking reaction, i.e. cure, is usually based on heat flow measurement by DSC, which is proportional to both overall heat release and cure rate according to Equation 9:[169,170]

$$\frac{dQ}{dt} = Q_{cure}\frac{d\alpha}{dt} = Q_{cure}k(T)f(\alpha), \tag{9}$$

where dQ/dt is the heat flow, t is the time, Q_{cure} is the total heat released when an uncured sample is brought to complete cure, $d\alpha/dt$ is the cure rate, α is the extent of monomer conversion to a crosslinked network, $k(T)$ is the Arrhenius rate constant and $f(\alpha)$ is the reaction model. The extent of cure, α, is determined by integrating the heat flow curve. The temperature dependence of the rate constant is introduced by replacing $k(T)$ with the Arrhenius equation, which gives

$$\frac{d\alpha}{dt} = Ae^{(\frac{-E}{RT})} f(\alpha). \quad (10)$$

The pre-exponential factor, A, and the activation energy, E, are traditionally determined from isothermal experiments, converting Equation 10 to logarithmic form Equation 11 to solve A and E:

$$\log_{10} k = \log_{10} A - \frac{E}{2.303RT}. \quad (11)$$

The determination of activation energy is an important objective of any kinetic investigation. However, if activation energy is determined according to the procedure presented above, the result is a single set of global Arrhenius parameters for the whole process. This means that the simulation of multi-step reactions is problematic. The model-free approach allows the apparent activation energy to be determined as a function of the extent of conversion and/or temperature without assuming a particular form of the reaction model. For nonisothermal conditions, when the temperature varies with time with a constant heating rate, $\beta = dT/dt$, Equation 10 can be rewritten as in Equation 12:

$$\frac{d\alpha}{dT} = \frac{A}{\beta} e^{(\frac{-E}{RT})} f(\alpha). \quad (12)$$

Too often the data is forced to fit to the single-step kinetic taking $f(\alpha)$ in one of its various reported forms.[171] Unfortunately, the use of an improper model can seriously violate the outcome of a reaction kinetic evaluation.[172] For the epoxy cure, the reaction order model, $(1-\alpha)^n$, and the autocatalytic cure model, $\alpha^m(1-\alpha)^n$, are the most frequently used. However, it is generally accepted that the epoxy cure is a multi-step reaction that likely involves several reaction mechanisms and/or reaction rate limiting stages with different sets of Arrhenius parameters.

Conventional isoconversional methods assume that the reaction rate at constant extent of conversion is only a function of the temperature. This holds for single-step reactions providing that the heating rates are not extreme. For multi-step reactions, activation energy can vary depending on the heating rate and the subsequent reaction path, thus leading to different extent of conversion. The differential method proposed by Friedmann[173] may result in erroneous values of activation energies because of poor resistance to experimental noise. The use of the integral methods proposed by Ozawa,[174] and Flynn and Wall[175] is preferred, therefore.[176] However, the integral methods also

require corrections.[177] To overcome the inaccuracies of the conventional approximation routines associated with the isoconversional methods,[173-175] Vyazovkin[178] developed a non-linear approximation method for the temperature integral. Vyazovkin and Sbirrazzuoli[176] calculated for a set of *n* experiments, carried out at different but constant heating rates, the minimum of the function

$$\sum_{i=1}^{n}\sum_{j\neq i}^{n}\left[\frac{I(E_\alpha,T_{\alpha,i})\beta_j}{I(E_\alpha,T_{\alpha,j})\beta_i}\right] \tag{13}$$

with

$$I(E_\alpha,T_\alpha)=\int_0^{T_\alpha} e^{\left(\frac{-E_\alpha}{RT}\right)}dT\,, \tag{14}$$

which must be evaluated numerically. In Equation 13, the indexes *i* and *j* denote different heating rates, *n* is the total number of heating rates, α is the conversion and *I* is the temperature integral. With this empirical method, the activation energy can be evaluated at any given value of α for multi-step kinetics.

The conversion-dependent apparent activation energies are obtained, by assuming a simple superposition of the individual reactions for a possible multi-step mechanism. It is also assumed that at the end of the reaction all the reactants have been converted to products with full conversion (α = 1). The process should not include simultaneously occurring exothermic and endothermic reactions or competing reactions, and it should not be partially diffusion controlled. With these boundary conditions taken into account, the advantages of the model-free analysis, i.e. simplicity and the avoidance of the erroneous choice of a kinetic model, can be put to use. Despite the evident benefits of the model-free analysis, there is an ongoing debate about the theoretical justification.[179-184] Although there is no agreement about the exact physical foundation of the approach, application has produced viable results and model-free analysis is gaining increasing acceptance as the thermal analysis community actively debates the best way to determine the reaction kinetics of complex systems.[135,179-185]

5 SUMMARY OF THE THESIS

The objective of the present work was to obtain a better understanding of interfacial compatibility, which is one of the major reliability-related concerns of advanced electronics. Materials were modified and characterised, and test specimens with representative interfaces were built up, tested and investigated. Both surface and bulk modifications of materials were carried out. The modified surfaces were investigated by means of topographical and chemical analyses. The interfacial adhesion of coating/substrate systems composed of copper/polymer, polymer/copper or polymer/polymer was investigated in carefully designed adhesion tests. A critical assessment was made of the pull-off adhesion test and surface free energy evaluation methods to ensure the validity of the results. In addition, a novel method for polymer film characterisation was introduced and novel star-shaped poly(ε-caprolactone) oligomers were synthesised for reactive blending with SU8 epoxy to achieve the modification of certain bulk properties of the SU8.

This thesis consists of seven publications. The main results of each publication are summarised as follows:

In Publication I, entitled "Evaluation of the surface free energy of spin-coated photodefinable epoxy", we critically assessed models based on Young's equation, which are commonly used in the calculation of the surface free energy of solid polymers. Surface free energy was calculated by these models for the photodefinable epoxy (SU8), which was later studied in Publications II and VII. The geometric mean model was found to have the most solid theoretical foundation and it was used in all later work. The interfacial adhesion between successive SU8 layers was determined by a pull-off method. Although it was later noticed that careful optimisation is needed for the reliable determination of interfacial adhesion, relative values of the adhesion strength provided useful information about the interfacial adhesion at the polymer/polymer interface.

Publication II, entitled "Pull-off test in the assessment of adhesion at printed wiring board metallisation/epoxy interface", sought a detailed understanding of the pull-off adhesion test method. The hypothesis of the study was that the use of a rigid support together with photodefinition of an adhesion test pad onto the coating to be studied would result in a more uniform stress distribution within the specimen than that provided by direct application of the method according to the ASTM D4541-95e1 standard. The standard does not require a rigid support or photodefinition. By combining mechanical modelling with careful experimental adhesion testing, we were able to show the influence of the properties of substrate on the measured adhesion strength. We demonstrated that if a flexible substrate is used rather than a rigid one, the adhesion strength is severely underestimated. In addition, the test area should be prepared to match in size the stud area of the test

equipment. This is not made clear in the literature, and often the test is carried out from an arbitrary place on the coating. If the test pad is not defined, however, the load applied to the set-up during the adhesion test will cause the stress concentration to appear at the wrong interface. With the help of these observations, we were able explain contradictory results reported in the literature. Moreover, we observed interfacial fractures, rather than cohesive bulk fractures, at higher values of the adhesion strength than have been reported earlier for the bulk fracture of the copper/SU8 system. Finally, we used the pull-off test to obtain information about differently aged samples and found that adhesion promoter enhanced the durability of the interfacial adhesion in environmental exposures and that properly pre-treated copper is relatively reliable without any other treatment.

In publications III-V, entitled "Surface modification and characterisation of photodefinable epoxy/copper systems", "Effects of surface treatments on adhesion of copper to a hybrid polymer material" and "Surface modification of a liquid crystalline polymer for copper metallization", we studied the interfacial adhesion of electroless and sputter-deposited copper to different polymer substrates. By employing contact angle measurements and surface free energy evaluations along with XPS analyses and topographical investigations of modified polymer surfaces before the adhesion test, and after it carrying out SEM examination of the fracture surface, we were able to deduce the adhesion mechanisms at the coating/substrate interfaces. The improvement of interfacial adhesion was experimentally verified by a modified pull-off test. The increase in surface free energy correlated well with the increase in adhesion strength of sputter-deposited copper. Nevertheless, there was poor correlation between the surface free energy of a polymer and the achieved adhesion strength with electroless copper. We concluded that electroless copper demands an effectively roughened surface with a sufficient number of microcavities for the formation of mechanical interlocking between the polymer and copper. Sputter-deposited copper, in turn, showed better interfacial adhesion to a relatively smooth surface with an appropriately modified surface chemistry, i.e. rich in oxygen or nitrogen functional groups. The studies did not, however, include experiments to determine if the sputter-deposited copper had penetrated into the polymer during the deposition process. The possibility of diffusion as an adhesion mechanism that provided the improved adhesion strength, when using sputter-deposition, cannot therefore be excluded.

Publication VI, entitled "Synthesis, characterisation and crosslinking of functional star-shaped poly(ε-caprolactone)", describes the synthesis of novel star-shaped low-molecular-weight polymer modifiers. With the help of controlled polymer structure tailoring we were able to synthesise reactive, i.e. crosslinkable, oligomers with different functional groups. Characterisation of the oligomers was carried out by $^{1}H/^{13}C$ nuclear magnetic resonance (NMR) spectroscopy, size exclusion chromatography (SEC), Fourier transform infrared (FTIR) spectroscopy and differential

scanning calorimetry (DSC). Among other things, the six-armed star-shaped structure was established. The polymer was further functionalised to contain a carbon-carbon double bond at the end of each branch to enable crosslinking without the need of a crosslinking agent. The crosslinking was induced either thermally with the use of peroxides or photochemically with the use of photosensitive initiator. The crosslinked polymer networks were characterised by Soxhlet extraction, DSC and FTIR, which showed that a high degree of crosslinking was achieved and that an itaconic double bond was much more reactive than the maleic double bond.

In Publication VII, entitled "Reactive blending approach to modify spin-coated epoxy film" we applied the knowledge obtained in the synthesis of the star-shaped polymer.[VI] Now we used saturated carboxylic acid functionalisation and prepared an oligomeric network precursor with a four-armed structure. This modification enabled reactive blending with epoxy by a dual-catalysed reaction, and various bulk as well as surface properties could be tailored simultaneously. With the help of model-free kinetic analysis we were able to adjust the crosslinking conditions to ensure dense crosslinking. This minimised the reaction induced phase separation while maximising the amount of incorporated oligomer. Finally, we demonstrated the use of a novel non-destructive method, spectrophotometry, in the determination of glass transition temperature and the out-of-plane thermal expansion of polymer films *in-situ* from silicon wafers. In addition, the spectrophotometry provided information about the optical properties of the modified polymers, which strongly suggested that the materials could be used in the manufacturing of optical waveguides.

References

1. Coombs, C.F. Editor, Printed circuit board handbook, 5th Ed., McGraw-Hill, New York 2001.
2. Harper, C.A. Editor, High performance printed circuit boards, McGraw-Hill, New York 2000.
3. Gonzalez, C.G., Wessel, R.A, Padlewski, S.A. IEEE T Adv Packaging 1999,22(3),385.
4. Holden, H. Micro IEEE 1998,8(4),10.
5. Zhang, S., De Baets, J., van Calster, A. Microelectron Reliab 1999,39,1337.
6. Li, W., Tummala, R. P-4 process. A novel high-density, low-cost multilayer planar thin-film PWB technology, In Proc 48th IEEE Electronic Components and Technology Conf, Seattle, WA, May 1998,151.
7. Neuberger, D., Jacobus, D., Lenihan, T., Robinson, C., Matijasevic, G., Ha, L., Gallagher, C., Castello, C., Gandhi, P. A new interlayer interconnect technology for multilayer fabrication, In Proc 7th IEEE Int Conf on Multichip Modules and High Density Packaging, Denver, CO, April 1998,218.
8. Kujala A., Tuominen R., Kivilahti J.K. Solderless interconnection and packaging technique for embedded active components. In Proc 49th Electronic Component Technology Conf, San Diego, CA, USA, June 1999,155.
9. Tuominen, R., Kivilahti, J.K. A novel IMB technology for integrating active and passive components, In Proc 4th Int Conf Adhesive Joining & Coating Technology in Electronics Manufacturing, Editor Hyytiäinen, M. (Institute of Electrical and Electronic Engineers, NY, 2000),269.
10. Waris, T.F., Tuominen, R., Kivilahti, J.K. Panel-sized integrated module board manufacturing**,** In Proc 1st Int IEEE Conf Polymers and Adhesives in Microelectronics and Photonics, Editors Kruse, N., Nieland, C., Wenzel, R. (IEEE, Piscataway, NJ, 2001),218.
11 Waris, T.F., Turunen, M.P.K., Laurila, T., Kivilahti, J.K., Evaluation of NiP integral resistors electrolessly deposited on flexible polyimide substrate, Microelectron Reliab in press.
12. Kivilahti, J.K., Liu, J., Morris, J.E., Suga, T., Wong, C.P. Panel-size component integration (PCI) with molded liquid crystal polymer (LCP) substrates, In Proc 52nd IEEE Electronic Component and Technology Conf., Editors McShane, M., Bezuk, S. (IEEE, Piscataway, NJ, 2002),955.

13. Brown, W.D. Editor, Advanced electronic packaging with emphasis on multichip modules, IEEE Press, New York 1999.
14. Griese, E. IEEE T Adv Packaging 2001,24,375.
15. Liu, Y.S., Wojnarowski, R.J., Hennessy, W.A., Rowlette, J., Stack, J., Kadar-Kallen, M., Green, E., Liu, Y., Bristow, J.P., Peczalski, A., Eldada, L., Yardley, J., Osgood, R.M., Scarmozzino, R., Lee, S.H., Patra, S. High density optical interconnects for board and backplane applications using VCSELs and polymer waveguides, In Proc 47th IEEE Electronic Component and Technology Conf. Editor Vardaman, E.J. (IEEE, Piscataway, NJ, 1997),391.
16. Schmieder, K., Wolter, K.-J. Electro-optical printed circuit board (EOPCB), in Proc 50th IEEE Electronic Component and Technology Conf., Editors Reynolds, T.G., III, McShane, M. (IEEE, Piscataway, NJ, 2000),749.
17. Houbertz, R., Domann, G., Cronauer, C., Schmitt, A., Martin, H., Park, J.-U., Fröhlich, L., Buestrich, R., Popall, M., Streppel, U., Dannberg, P., Wächter, C., Bräuer, A. Thin Solid Films 2003,442,194.
18. Immonen, M., Karppinen, M., Kivilahti, J.K. Fabrication and characterisation of optical polymer waveguides, Oral presentation at Polytronic III Conf, Montreux, Switzerland, Oct. 2003,91.
19. Turunen, M.P.K., Immonen, M., Kivilahti, J.K. Evaluation of the environmental reliability of polymer waveguides fabricated on printed wiring board, Poster presentation at Polytronic III Conf, Montreux, Switzerland, Oct. 2003,129.
20. Musikant, S. Optical materials: An introduction to selection and application, Marcel Dekker, New York, 1985.
21. Rogers, A. Essentials of optoelectronics with applications, Chapman & Hall, London 1997.
22. Ge J., Kivilahti, J.K. J Appl Phys 2002,92,3007.
23. Brewis, D.M., Briggs, D. Editors, Industrial adhesion problems. Oxford: Orbital Press; 1985.
24. Puligandla, V., Singh, P. Failure modes and mechanisms in electronic packages, Chapman and Hall, New York 1998.
25. Savolainen, P. Solder-filled anisotrotropic conductive adhesives in electronic interconnections, Helsinki University of Technology, Doctoral thesis, 1996.
26. Rimdusit, S., Ishida, H. Polymer 2000,41(22),7941-7949.
27. Kim, H.K., Shi, F.G. Microelectr Journal 2001,32(4),315-321.
28. Stepniak, F. Microelectron Reliab 2004,44,805.

29. He, Y., Moreira, B.E., Overson, A., Nakamura, S.H., Bider, C., Briscoe, J.F. Thermochim Acta 2000,357-358,1.
30. Okura, J.H., Shetty, S., Ramakrishnan, B., Dasgupta, A., Caers, J.F.J.M., Reinikainen, T. Microelectron Reliab 2000,40,1173.
31. Labbé, P., Donval, A., Hierle, R., Toussaere, E., Zyss, J. CR Phys 2002,3(4),543.
32. Kinloch, A.J., Little, M.S.G., Watts, J.F. Acta Mater 2000,48,4543.
33. Park, C.E., Han, B.J., Bair, H.E. Polymer 1997,38(15),3811.
34. Sham, M.-L., Kim, J.-K. J Adhesion Sci Technol 2003,17,1923.
35. Luo, S., Wong, C.P. IEEE T Electron Pack 2003,26(4),345.
36. Lee, H.-Y., Kim, S.-R. J Adhesion Sci Technol 2002,16,621.
37. Nguyen, L.T., Lo, R.H.Y., Chen, A.S., Belani, J.G. IEEE T Reliab 1993,42,518.
38. Chang, S.-J., Hwang, S.-J. IEEE T Electron Pack 2003,26(4),281.
39. Weigl, B.H., Bardell, R.L., Cabrera, C.R. Adv Drug Deliv Rev 2003,55,349.
40. Krawczyk, S. Phys Stat Sol C 2003,3,998.
41. Becker, H, Locascio, L.E. Talanta 2002,56,267.
42. Becker, H., Gärtner, C. Rev Molec Biotech 2001,82,89.
43. Tirrell, M., Kokkoli, E., Biesalski, M. Surf Sci 2002,500,61.
44. Hiljanen-Vainio, M.P., Orava, P.A., Seppälä, J.V. J Biomed Mater Res 1997,34,39.
45. Helminen, A., Kylmä, J., Tuominen, J., Seppälä, J.V. Polym Eng Sci, 2000,40,1655.
46. Gao, C., Yan, D. Prog Polym Sci 2004,29,183.
47. Voit, B.I. CR Chim 2003,6,821.
48 Turunen, M.P.K., Synthesis and characterisation of crosslinked biodegradable polyester, Master's Thesis, Helsinki University of Technology, 1999.
49. Gabriel, C., Kokko, E., Löfgren, B., Seppälä, J., Münstedt, H. Polymer 2002,43,6383.
50. Ratna, D., Simon, G.P. Polymer 2001,42,8833.
51. Chandrasekhar, A., Brebels, S., Stoukatch, S. Beyne, E., De Raedt, W., Nauwelaers, B. Microelectron Reliab 2003,43,351.
52. Wu, S. Polymer interface and adhesion, Marcel Dekker, New York, 1982.
53. Efremov, M.Y., Olson, E.A., Zhang, M., Allen, L.H. Thermochim Acta 2003,403,37.
54. Zhou, H., Kim, H.K., Shi, F.G., Zhao, B., Yota, J. Microelectr Journal 2002,33,221.
55. Dinelli, F., Buenviaje, C., Overney, R.M. Thin Solid Films 2001,396,138.
56. Jiang, X., Yang, C.Z., Tanaka, K., Takahara, A., Kajiyama, T. Phys Lett A 2001,281,363.
57. Forrest, J.A., Dalnoki-Veress, K., Stevens, J.R., Dutcher, J.R. Phys Rev Lett 1996,77,2002.
58. van Zanten, J.H., Wallace, W.E., Wu, W.-I. Phys Rev Lett 1996,53,R2053.

59. Lovejeet, S., Ludovice, P.J., Henderson, C.L. Thin Solid Films 2004,449,231.
60. Fukao, K., Miyamoto, Y. Europhys Lett 1999,46,649.
61. Arefi-Khonsari, F., Kurdi, J., Tatoulian, M., Amouroux, J. Surf Coat Tech 2001,142-444,437.
62. Zaporojtchenko, V., Strunskus, T., Behnke, K., Bechtolsheim, C., Thran, A., Faupel, F. Microelectron Eng 2000,50(1-4),465.
63. Faupel, F., Willecke, R., Thran, A. Mat Sci Eng R 1998,22(1),1.
64. Opila, R.L., Eng, J. Prog Surf Sci 2002,69(4-6),125.
65. Faupel, F., Gupta, D., Silverman, B.D., Ho, P.S. Appl Phys Lett 1989,55(4),357.
66. Aveyard, R., Haydon, D.A. An introduction to the principles of surface chemistry, Cambridge University Press, Cambridge, 1973.
67. Adamson, A.W. Physical chemistry of surfaces, 5th edition, John Wiley & Sons Inc, New York, 1990.
68. Gastellan, G.W. Physical chemistry, 2nd edition, Addison-Wesley Publishing Company, Massachusetts, 1971.
69. Defay, R., Prigogine, I., Bellemans, A., Everett, D.H. Surface tension and adsorption, Longmans, Green & Co LTD, London, 1966.
70. Tartaglino, U., Passerone, D., Tosatti, E., Di Tolla, F. Surf Sci 2001,482-485,1331.
71. Good, R.J., Stromberg, R.R. Editors, In Techniques of measuring contact angles, surface and colloid science, Plenum: New York, 1979.
72. Lee, L.H. Editor, In Adhesion science and technology, polymer science and technology, Plenum: New York, 1975.
73. Wolansky, G., Marmur, A. Colloid Surface A 1999,156(1-3),381.
74. Palasantzas, G., de Hosson, J. Th. M. Acta Mater 2001,49,3533.
75. Uelzen, Th., Müller, J. Thin Solid Films 2003,434(1-2),311.
76. Cassie, A.B.D., Baxter, S. Trans Farad Soc 1944,40,546.
77. Israelivich, J.N., Gee, M.L. Langmuir 1989,5,288.
78. Hofer, R., Textor, M., Spencer, N.D. Langmuir 2001,17,4123.
79. Chibowski, E. Adv Colloid Interfac 2003,103(2),149.
80. Kim, J.S., Friend, R.H., Cacialli, F. J Appl Phys 1999,86(5),2774.
81. Extrand, C.W. J Colloid Interf Sci 2002,248(1),136.
82. Lam, C.N.C., Kim, N., Hui, D., Kwok, D.Y., Hair, M.L., Neumann, A.W. Colloid Surface A 2001,189(1-3),265.
83. Weh, L. Mat Sci Eng C 1999,8–9,463.

84. Lu, X.F., Hay, J.N. Polymer 2001,42(19),8055.
85. Aida, S., Sakurai, S., Nomura, S. Polymer 2002,43(9),2881.
86. Cubaud, T., Ferminger, M. J Colloid Interf Sci 2004,269,171.
89. Breisch, S., de Heij, B., Löhr, M., Stelzle, M. J Micromech Microeng 2004,14,497.
88. Park, C., Yoon, J., Thomas, E.L. Polymer 2003,44(22),6725.
89. de Gennes, P.G. Rev Mod Phys 1985,57(3),827.
90. Yost, F.G., Sackinger, P.A., O'Toole, E.J. Acta Mater 1998,46(7),2329.
91. Kalogeropoulou, S., Rado, C., Eustathopoulos, N. Scripta Mater 1999,41(7),723.
92. Yost, F.G., Hosking, F.M., Frear, D.R. Editors, In The mechanics of solder alloy wetting and spreading, Van Nostrand Reinhold, New York, 1993.
93. Wang, J. Microelectron Reliab 2002,42,293.
94. Alteraifi, A.M., Sherif, D., Moet, A. J Colloid Interf Sci 2003,264(1),221.
95. Tanner, L.H. J Phys D Appl Phys 1975,12(9),1473.
96. Seaver, A., Berg, J. J Appl Polym Sci 1994,52,431.
97. Wasan, D.T., Nikolov, A.D., Brenner, H. Science 2001,291,605.
98. Breslauer, E., Troczynski, T. Mat Sci Eng A 2001,302,168.
99. Mittal, K.L. Editor, Adhesion measurement of films and coatings. Utrecht, The Netherlands: VPS, 1995.
100. Kinloch, A.J. Adhesion and adhesives: science and technology. London: Chapman and Hall, 1987.
101. Kinloch, A.J. J Mater Sci 1982,17,617.
102. Valli, J. J Vac Sci Technol A 1986,4(6),3007.
103. Kafkalidis, M.S., Thouless, M.D. Int J Solids Struct 2002,39,4367.
104. Rekners, U., Kalnins, M. Prog Org Coat 2000,38,35.
105. Ollendorf, H., Schneider, D. Surf Coat Tech 1999,113,86.
106. Kinloch, A.J. Editor, Durability of structural adhesives, Elsevier Applied Science, London, 1983.
107. Gledhill, R.A., Kinloch, A.J., Shaw S.J. J Adhesion 1977,9(1),81.
108. Martin, P.L. Editor, Electronic failure analysis handbook, McGraw Hill, New York, 1999.
109. Bowditch, M.R. Int J Adhesion Adhes 1996,16,73.
110. Abbott, W.H., Neer, J.H., Healey, H.J. Effects of test procedures and sequences on the performance of tin-plated connectors. In Proc 39th IEEE Holm Conf Electrical Contacts. Sept 1993,191.
111 Schröer, D., Nichols, R.J., Meyer, H. Electrochim Acta 1995,40,1487.

112 Roizard, X., Wery, M., Kirmann, J. Composite Structures 2002,56,223.
113 Chu, P.K., Chen, J.Y., Wang, L.P., Huang, N. Mater Sci Eng R 2002,36,143.
114 Richter, K., Orfert, M., Drescher, K. Surf Coat Tech 1997,97,481.
115 Wang, Z., Li, H., Shodiev, H., Suni, I.I. Electrochem Solid State Lett 2004,7,C67.
116 Chang, C.Y., Sze, S.M., Editors, In ULSI technology, McGraw-Hill, New York, 1996.
117 Miura, S., Honma, H. Surf Coat Tech 2003,169-170,91.
118. Ge, J., Tuominen, R., Kivilahti, J.K. J Adhesion Sci Technol 2001,15(10),1133.
119. Sawyer, L.C., Grubb, D.T., Polymer microscopy, 2nd Edn, Chapman & Hall, London 1996.
120. Goldstein, J.I., Romig, A.D. Jr., Newberry, D.E., Lyman, C.E., Echlin, P., Fiori, C., Joy, D.C., Lifshin, E., Scanning electron microscopy and X-ray microanalysis, 2nd Edn, Plenum, New York, 1992.
121. Vezie, D.L., Thomas, E.L., Adams, W.W. Polymer 1995,36(9),1761.
122. Binning, G. Rohrer, H., Gerber, Ch., Weibel, E. Phys Rev Lett 1982,49,57.
123. Binning, G., Quate, C.F., Gerber, Ch. Phys Rev Lett 1986,56,930.
124. Jandt, K.D. Mat Sci Eng R 1998,21,221.
125. Zhong, Q., Inniss, D., Kjoller, K., Elings, V.B. Surf Sci 1993,290(1-2),L688.
126. Siau S., Vervaet A., Schacht E., van Calster A. J Electrochem Soc 2004,151(2),C133.
127. Duwez, A.-S. J Electron Spectrosc 2004,134,97.
128. Dufrene, Y.F., Marchal, T.G., Rouxhet, P.G. Appl Surf Sci 1999,144–145,638.
129. Pigois-Landureau, E., Nicolau, Y.F., Delamar, M. Synthetic Met 1995,72,111.
130. Dybowski, C., Lichter, R.L. Editors, NMR spectroscopy techniques, Marcel Dekker, New York, 1987.
131. Dyke, S.F., Floyd, A.J., Sainsbury, M., Theobald, R.S., Organic spectroscopy: An introduction, 2nd Ed., Longman Group Ltd., London, 1978
132. Fessenden, R.J., Fessenden, J.S., Organic chemistry, 5th Ed., Brooks/Cole, Belmont, 1993.
133. Skoog, D.A., Holler, F.J., Nieman, T.A., Principles of instrumental analysis, 5th Ed., Brooks/Cole, London, 1998.
134. Kostanski, L.K., Keller, D.M., Hamielec, A.E. J Biochem Biophys Methods 2003,58(2),159.
135. Galwey, A.K. Thermochim Acta 2004,413,139.
136. Hertzberg, R.W. Deformation and fracture mechanics of engineering materials, John Wiley & Sons: New York, 1989.
137. Ylinen, A., Elasticity and strength of materials I (in Finnish), WSOY, Porvoo, 1965.

138. Menard, K.P. Dynamic mechanical analysis: A practical introduction, CRC Press: Boca Raton, 1999.
139. US Patent 5,999,267 (December 1999).
140. Jelison, G.E., Modine, F.A. Appl Phys Lett 1996,69(3),371.
141. Jelison, G.E., Modine, F.A. Appl Phys Lett 1996,69(14),2137.
142. Schroder, D.K. Semiconductor materials and device characterization, John Wiley & Sons: New York, 1998.
143. Barradas, N.P., Keddie, J.L., Sackin, R. Phys Rew E 1999,59(5),6138.
144. Kahle, O., Wielsch, U., Metzner, H., Bauer, J., Uhlig, C., Zawatzki, C. Thin Solid Films 1998,313-314,803.
145. See, Y.K., Cha, J., Chang, T., Ree, M. Langmuir 2000,16,2351.
146. Reiter, G. Macromolecules 1994,27,3046.
147. Raptis, I., Diakoumakos, C.D. Microelectr Eng 2002,61-62,829.
148. Zhang, J., Zhang, R., Chen, H., Li, Y., Wu, Y.C., Suzuki, R., Sandreckski, T.C., Ohdaira, T., Jean, Y.C. Radiat Phys Chem 2003,68,535.
149. Beaucage, G., Composto, R., Stein, R. S. J Polym Sci Pol Phys 1993,31,319.
150. Beach, E.R., Tormoen, G.W., Drelich, J. J Adhesion Sci Technol 2002,16(7),845.
151. Planinšek, O., Trojak, A., Srčič, S. Int J Pharm 2001,221,211.
152. Carlon, E., van Beijeren, H. Phys Rev E, 2000,62,7646.
153. Berry, M.V., Durrans, R.F., Evans, R. J Phys A Gen Phys 1972,5,166.
154. Potvin, J., Rebbi, C. Phys Rev Lett 1989,62,3062.
155. Changa, Y.A., Chen, S., Zhang, F., Yan, X., Xie, F., Schmid-Fetzerd, R., Oates, W.A. Prog Mat Sci 2004,49,313.
156. Kwok, D.Y., Neumann, A.W. Colloids Surf A 2000,161,31.
157. Fox, H.W., Zisman, W.A. J Colloid Sci 1950,5,514.
158. Wu, S. J Polym Sci Pol Phys 1971,34,19.
159. Fowkes, F.M. J Phys Chem 1963,67,2538.
160. Mittal, K.L., Anderson, V.R., Jr. Editors, In Acid–base interactions, VPS, Utrecht, The Netherlands, 1991.
161. Owens, D.K., Wendt, R.C. J Appl Polym Sci 1969,13,1741.
162. Kaelble, D.H., Uy, K. C. J Adhes 1970,2,50.
163. van Oss, C.J., Good, R.J., Chaudhury, M. K. Langmuir 1988,4,884.
164. van Oss, C.J., Good, R.J., Chaudhury, M. K. J Colloid Interf Sci 1986,111,378.
165. van Oss, C.J., Chaudhury, M. K., Good, R. J. Chem Rev 1988,88,927.

166. Johnson, R.E., Dettre, R.H. Langmuir 1989,5,293.
167. Makkonen, L. Langmuir 2000,16,7669.
168. Decker, E.L., Garoff, S. Langmuir 1996,12,2100.
169. Flynn, J.H. J Thermal Anal 1990,36,1579.
170. Ninan, K.N. J Thermal Anal 1989,35,1267.
171. Zhou, D., Schmitt, E.A., Zhang, G.G.Z., Law, D., Wight, C.A., Vyazovkin, S., Grant, D.J.W. J Pharm Sci 2003,92,1367.
172. Vyazovkin, S., Wight, C.A. Thermochim acta 1999,340-341,53.
173. Friedmann, H. J Polym Sci Pol Phys 1963,6,183.
174. Ozawa, T. Bull Chem Soc Jap 1965,38,1881.
175. Flynn, J.H., Wall, L.A. J Res Nat Bur Standards 1996,70A,487.
176. Vyazovkin, S., Sbirrazzuoli, N. Macromol Chem Phys 1999,200(10),2294.
177. Flynn, J.H. J Therm Anal 1983,27,95.
178. Vyazovkin, S. J Comput Chem 1997,18,393.
179. Flynn, J.H. J Thermal Anal 1988,34,367.
180. Brown, M.E. J Thermal Anal 1997,49,17.
181. Maciejewski, M., Reller, A. Thermochim Acta 1987,110,145.
182. Sewry, J.D., Brown, M.E. Thermochim Acta 2002,390,217.
183. Opfermann, J.R., Flammersheim, H.-J. Thermochim Acta 2003,397,1.
184. Vyazovkin, S. Thermochim Acta 2003,397,269.
185. Brown, M.E., Maciejewski, M., Vyazovkin, S., Nomen, R., Sempere, J., Burnham, A., Opfermann, J., Strey, R., Anderson, H.L., Kemmler, A., Keuleers, R., Janssens, J., Desseyn, H.O., Li, C.-R., Tang, T.B., Roduit, B., Malek, J., Mitsuhashi, T. Thermochim Acta 2000,355,125.